Strategy for Identification of Nanomaterials' Critical Properties Linked to Biological Impacts: Interlinking of Experimental and Computational Approaches

Iseult Lynch, Antreas Afantitis, Georgios Leonis, Georgia Melagraki and Eugenia Valsami-Jones

Abstract Significant progress has been made over the last 10 years towards understanding those characteristics of nanoscale particles which correlate with enhanced biological activity and/or toxicity, as the basis for development of predictive tools for risk assessment and safer-by-design strategies. However, there are still a number of disconnects in the nanosafety workflow that hamper rapid progress towards full understanding of nano-specific mechanisms of action and nanomaterials (NMs)-induced adverse outcome pathways. One such disconnect is between physico-chemical characteristics determined experimentally as part of routine NMs characterisation, and the ability to predict a NM's uptake and impacts on biological systems based on its pristine physico-chemical characteristics. Identification of critical properties (physico-chemical descriptors) that confer the ability to induce harm in biological systems *under the relevant exposure conditions* is central, in order to enable both prediction of impacts from related NMs [via quantitative property-activity or structure-activity relationships (QPARs/QSARs)] and

I. Lynch (✉) · E. Valsami-Jones
School of Geography, Earth and Environmental Sciences University of Birmingham, Birmingham B15 2TT, UK
e-mail: i.lynch@bham.ac.uk

E. Valsami-Jones
e-mail: E.ValsamiJones@bham.ac.uk

A. Afantitis · G. Leonis · G. Melagraki (✉)
Novamechanics Ltd., Nicosia, Cyprus
e-mail: melagraki@novamechanics.com; melagraki@insilicolab.eu

A. Afantitis
e-mail: afantitis@novamechanics.com

G. Leonis
e-mail: leonis@novamechanics.com

A. Afantitis · G. Melagraki
InSilicoLab L.P., Athens, Greece

K. Roy (ed.), *Advances in QSAR Modeling*, Challenges and Advances in Computational Chemistry and Physics 24, DOI 10.1007/978-3-319-56850-8_10

development of strategies to ensure that these features are avoided in NM production in the future ("safety by design"). For this purpose, we have launched the Enalos InSilico platform, which is dedicated to the dissemination of our developed in silico workflows for NM risk assessment. So far, two predictive models have been made available online. The first tool is a Quantitative Nanostructure-Activity Relationship (QNAR) model for the prediction of the cellular uptake of NMs in pancreatic cancer cells and the second is an online tool for in silico screening of iron oxide NMs with a predictive classification model for their toxicological assessment.

Keywords Nanomaterial characterization · Physico-chemical/structural properties · Data mining · Machine learning for nanomaterial data · Quantitative Nanostructure-Activity Relationship (QNAR)

List of Abbreviations

AOP	Adverse Outcome Pathway
BSAI	Biological Surface Adsorption Index
CCC	Critical Coagulation Concentration
EU	European Union
HOMO	Highest Occupied Molecular Orbital
LUMO	Lowest Unoccupied Molecular Orbital
MIE	Molecular Initiating Event
NM	Nanomaterial
NP	Nanoparticle
PS-NH_2	Amino-functionalized polystyrene
PZC	Point of Zero Charge
QNAR	Quantitative Nanomaterial-Activity Relationship
QPAR	Quantitative Property-Activity Relationship
QSAR	Quantitative Structure-Activity Relationship
ROS	Reactive Oxygen Species
TEM	Transmission Electron Microscopy

1 Introduction

Nanomaterials (NMs) are a highly diverse group of chemicals, defined mainly by their small size, which ranges from 1 to 100 nm, but varying enormously regarding their physico-chemical properties, such as composition, shape, surface charge, crystallinity, and reactivity, among others (Stamm 2011). Researchers in the field of NM science are struggling to associate the primary properties of NMs with their biological reactivity and toxicity (Valsami-Jones 2015; Nel 2015), as well as formulating appropriate methodologies to understand and utilize them to their full potential. Due to the widespread application and commercial usefulness of NMs in

products ranging from industrial to consumer goods (Tsuzuki 2009), it is necessary to view NMs from a regulatory perspective. However, this is particularly challenging, in part because methods to identify many of the important physico-chemical properties are lacking, or are not yet sufficiently validated (von der Kammer et al. 2012). Consequently, there is an extensive literature indicating that only size measurements are currently reliable to establish a regulatory definition of NMs (Linsinger 2012). Three main NM-associated concerns have been implicated in making regulation, read-across and impact prediction of NMs problematic: (1) the fact that many properties are non-scalable, (2) the need to distinguish between intrinsic versus extrinsic (i.e., context dependent) properties, (Lynch et al. 2014a) and (3) the fact that many properties are interlinked (e.g., changing one property may induce changes to another) which renders the description of property-activity relationships arduous and makes the development of systemic libraries of NMs challenging. These concerns are presented below in detail.

As part of continuing EU efforts to define NMs for regulatory purposes, the Joint Research Centre (JRC) of the European Commission have classified physico-chemical parameters of NMs into those that scale with size (scalable) and those that display unique nanoscale characteristics below a certain size (non-scalable) (Lövestam 2010). Examples of non-scalable properties include confinement effects, such as the broad HOMO-LUMO gap (or the related band gap) of semiconductor NMs that increases drastically for diameters below 5 nm, thermal properties, such as the exponential decrease of the melting point of In and Sn NMs below a diameter of 15 nm, and the solubility via dependence on the surface tension, which deviates significantly from the classical behaviour when particle sizes drop below 25 nm (Lövestam 2010). Size-dependent crystallinity also alters the interface properties of NMs, such as surface reaction rates, adsorption capacity, catalytic processes and redox potential, which control molecular processes that are related to diverse cell functions. The challenge is evident since non-scalable properties are material-dependent, and there is no straightforward, material-independent relation between particle size and properties or functions (Lövestam 2010).

In connection with the non-scalable parameters, several NM properties depend on the context in which they are studied, meaning that they are affected by the "environment". For example, the layer of biological molecules that surrounds certain NMs upon dispersion in a biological fluid has been implicated in conferring a "biological identity" (Walczyk 2010), which derives from the elemental synthetic identity, (Fadeel 2013) as this determines which biomolecules bind to the surface (e.g., through electrostatic and hydrophobic interactions, as well as favourable entropy contributions) (Dawson 2007). A critical article from Yang et al. outlines the relationship among NM surface properties, the properties of the surrounding medium (e.g., pH, ionic strength, salt composition) and the properties of the bio- or macro-molecules under study (Yang 2013). A related approach has been considered to describe and predict NM interactions in the natural environment, thus highlighting the ecological identity of NMs (Lynch et al. 2014a). A suggested classification framework assumed that NM toxicity can be predicted as the sum of three

"quantifiable" parameters (principal components). These parameters include the diversity of modes of action of NMs, and are classified as *intrinsic* properties (e.g., structural features), *extrinsic* properties (e.g., surface interactions, changes induced upon binding of biomolecules and other environmental interactions), and composition (Lynch et al. 2014b). Several NM physico-chemical properties belong to the intrinsic category (for example, strain which also includes shape, porosity, structure and HOMO-LUMO gap), and our consideration allows the construction of a scale depicting their relative contributions to this category. Similarly, conformational changes due to binding of biomolecules, such as protein unfolding, receptor activation, membrane damage, and fibrillation comprise the second category. Chemical composition is the third category and properties linked to the inherent molecular toxicity, charge, hydrophobicity and coating (also associated with both the intrinsic and extrinsic descriptions) are important (Lynch et al. 2014a). Table 1 provides an initial estimation of the key physico-chemical features that are considered crucial for NM toxicity, and whether they are likely to be context-dependent and thus require additional characterisation under the relevant exposure conditions as well as in the pristine form. The importance of such changes to the NMs properties and their adsorbed layers of biomolecules (the so-called biological and ecological identities of NMs), in terms of predicting NM uptake and toxicity is one of the key questions to be addressed by QSARs/QPARs currently. As yet however, limited attention has been paid to the physical transformations that NMs themselves undergo during, for example, environmental ageing (Lowry 2012) in terms of incorporation into QSARs.

The third challenge is the inter-dependency of many NM properties. Unfortunately, the exact relationships governing these interdependencies have yet to be established, in part due to the lack of available libraries of systematically varied individual NM properties. This would require property variation in a precise manner to identify crucial parameters driving toxicity, and to evaluate toxicity thresholds for various descriptors. However, the development of systematically varied NMs libraries is hampered by the fact that the variation of one property may inadvertently induce changes to several others, for example synthesis strategies to change the shape or length of a NM may require use of different templating molecules that result in differences in the surface chemistry of the particles also (Soler 2007; Bussy 2012; Zhang 2012b). This is illustrated in Fig. 1 for two different NMs (Au and ZnO, being typical examples of a metal and a soluble metal oxide, respectively), where the obviously interlinked properties are highlighted, although other inter-linkages likely also exist. This interdependence of physico-chemical properties also contributes to the inadequacy of the scientific efforts to date to obtain a set of agreed descriptors for NMs classification [even on a limited set of physico-chemical end-points against which to characterise NMs (see Stefaniak 2013 and discussion therein)].

The schematic representation (Fig. 1) shows some of the descriptor space that can, in principle, be varied through development of NM libraries and also demonstrates that (i) not all descriptors are relevant to all NM types, and (ii) not all parameters can be varied independently as in some cases the method used to vary

Table 1 Initial assessment of the potential context-dependent changes in physico-chemical properties of NMs

Parameter/Descriptor	Context dependent?	Potential impacts of surroundings
Size/Size distribution	Yes	In the environment, most likely decreased by binding of natural organic matter (stabilization). Protein binding may lead to either increased or decreased size via bridging or steric stabilisation
		pH/ionic strength may alter agglomeration
Surface area	Yes	Aggregation/agglomeration will reduce available surface area
Purity (particle/dispersant)	Maybe	Impurities/dispersants may be more effectively released from NM surface under different environmental conditions
Dissolution potential	Yes	pH, ionic strength, redox potential and adsorbed biomolecules affect dissolution rate
Photochemical activity	Most likely	Differences in pH and ionic strength and presence/absence of organic matter may affect electron transfer and result in protonation of different excited states
Surface charge/chemistry	Yes	Binding of ions/biomolecules may confer a different charge/charge distribution and surface groups but this may be dynamic
Hydrophobicity	Yes	Binding of biomolecules typically results in a more hydrophilic surface presentation, although may be dynamic
Redox activity	Most likely	Different surfaces/coatings/bound ligands may result in different radical species being generated (Li 2013)
Shape	Most likely	Agglomeration will result in different overall shape. Bundling/unbundling of nanotubes is an example
Crystal structure	Unlikely	Structure is a bulk property, established during the formation of an NM and cannot change by processes occurring on the surface, unless if the NM dissolves completely and re-precipitates
Porosity/Surface defects	Most likely	Though dependent on pore size or nature of defect, most likely decreased due to biomolecule absorption; may also be influenced by dissolution if NMs do not dissolve congruently or are a mixed phase

one parameter also changes another. The examples show gold (Au) NMs and ZnO NMs, which are used to represent easily versus poorly soluble NMs. In the example of Au NMs, several of the parameters are automatically ruled out as the atomic structure and subsequent packing of Au molecules does not result in particles with different crystal structures [at least at sizes beyond ~1 nm whereupon the cluster structure is templated into the particles (Wells 2015)]. In the example of ZnO NMs, it is clear that changing the capping agent will impact on dissolution potential, and surface properties such as charge and hydrophobicity, and thus the capping agent cannot be varied in insolation from other (interlinked) properties.

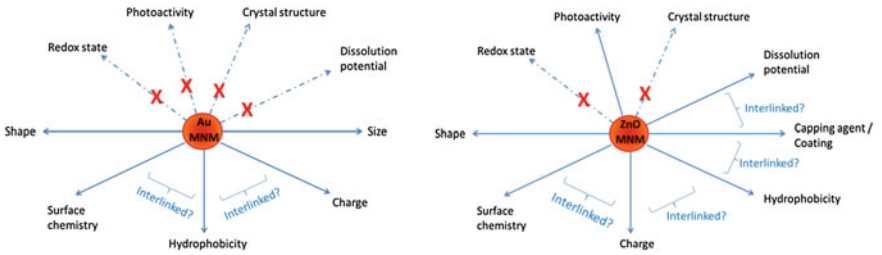

Fig. 1 Graphical presentation of the principles of NM library development and how systematic variation of one parameter can result in changes to other (interlinked) parameters

In addition to the direct interdependencies of physico-chemical properties, there is also the potential for additive (cooperative) or competitive effects in terms of how NMs properties result in interactions with, and impacts on, living systems. Enhanced binding to target cells using multiple physical and chemical interactions, and a range of distances where the addition of two effective repulsive interactions became an attraction, has been demonstrated (Nap 2013). Such models give insight into the competing and highly non-additive nature of different effective interactions in nanoscale systems in constrained environments, such as are ubiquitous in synthetic and biological systems, and suggest that these should be taken into account in the development of QNARs.

Besides the aforementioned NM challenges, there are also practical concerns among the diverse communities working with NMs to communicate with each other, regarding terminology, limitations of synthetic procedures, characterisation and modelling approaches, etc. as well realistic plans to produce the experimental results needed to underpin and validate models in the short and medium terms. Thus, there are two major obstacles regarding successful development of QNARs: (a) the lack of adequate and systematic experimental data (which requires high-quality systematically varied NM libraries) and (b) the currently limited knowledge on mechanisms of toxic action of NMs under realistic exposure and ageing conditions. Subsequent sections of this chapter offer insights into the current state of the art in terms of NM libraries and the QSARs that have been developed using these libraries, as well as the present understanding of the main physico-chemical properties of toxicological relevance (see also Table 1).

An understanding of the relationship between the physico-chemical properties of a particular NM and its in vitro and in vivo behaviour would provide the basic information for assessing toxic response and more importantly may yield predictive models for sub-classes of NMs allowing grouping of NMs in a similar manner to that applied for chemicals. Thus, we also outline current efforts to bridge the current disconnect between the modelling and experimental communities, and thereby to enhance progress. Among the successes listed so far are the development of a tool for surface chemistry, which is challenging experimentalists to re-think the way NMs and their surfaces are described and connect these with cellular uptake, and a

model for toxicity assessment of iron oxides with different core, coating and surface modifications.

Here, we propose a living classification system that incorporates the context-dependent evolution of several physico-chemical features of NMs (as shown in Table 1) and evolves continuously with new data generation and as new patterns emerge. Practically, this process may be likened to a modelling scheme, where the initial steps constitute a training process, populating it with data, which associate physico-chemical descriptors of NMs (including aged and biologically or environmentally transformed forms) with biological impacts. This would be the cornerstone for a second phase of testing the classification system against less well defined NMs to ensure that the predicted classifications match the data generated, and then following an approach where less and less experimental data is needed in order to evaluate classification and safety implications. This will produce a valuable set of tools for QSARs/QPARs and prediction of NM effects for risk assessment, regulation, and re-design of NMs synthesis according to the principles of safety by design to minimise the occurrence and effect of descriptors found to link directly to a toxicological mechanism or end-point as shown in Fig. 2.

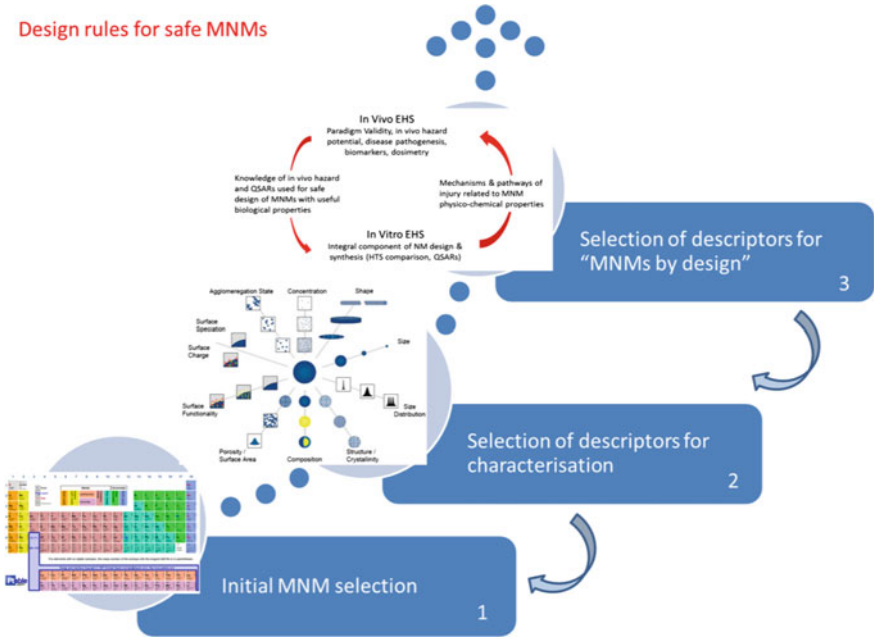

Fig. 2 Spiralling-type approach to NM classification, where earlier phases are "inspired" by tentative efforts at defining the later stages. *Note* graphical illustrations for stages 2 and 3 are from Hassellöv (2009) and Meng (2009), respectively

2 NM Physico-chemical Properties of Toxicological Relevance

The establishment of a safe nanotechnology necessitates the development of evaluation procedures to determine hazardous NM properties that could be modified to improve NM safety (George 2012).

(i) the release of toxic compounds from NMs (e.g., Cd from quantum dots)—i.e., **NM dissolution**;
(ii) the direct effects induced after physical contact with NMs, influenced by their size, shape and surface features, and which interfere with important biological functions—i.e., **NM interactions**; (so-called *extrinsic* factors)
(iii) the inherent features of the NM, such as photochemical and redox properties resulting from band gap or crystalline phase—i.e., **NM (surface) specific effects**; (so-called *intrinsic* factors), and
(iv) the capacity of NMs to act as transporters of toxic chemicals to sensitive tissues—i.e., **NM Trojan horse effects**.

Once a NM enters a cell, toxicity may occur via one or a combination of these mechanisms. Some toxicity patterns are also emerging; for example, positively charged NMs are generally more toxic than negatively charged NMs (Bexiga 2011; Pagnout 2012; Zheng 2013), although this is not always the case (Lee 2013; Merhi 2012).

Most physico-chemical properties from Table 1 are somehow related to toxicity in several of the mechanisms, however, the quantitative relationships between these properties and the biological uptake and toxicity are not yet clarified. Some examples of the four aforementioned mechanisms are presented below, with an emphasis on the physico-chemical properties, which have been implicated in direct associations with toxicity.

2.1 NM Dissolution

As a representative example of the first toxicity pathway, dissolution of ZnO NMs and subsequent Zn^{2+} release is known to induce cytotoxicity effects, with the mechanisms having recently been elucidated as reactive oxygen species (ROS) generation and activation of an integrated cytotoxic pathway, which involves intracellular calcium flux, mitochondrial depolarization, and plasma membrane leakage (George 2012). A recent seminal work has shown that ZnO cytotoxicity could be reduced by iron doping, which altered the material matrix to diminish Zn^{2+} release (George 2012). This study showed a workflow for identification of an NM descriptor of toxicological relevance, and also provided a strategy to "design out" the toxicity by Fe doping in order to reduce the ZnO NM dissolution potential.

While coating is a typical approach to slow or prevent NM dissolution, recent work has suggested that surface coating or passivation may itself affect the NM core, with more fundamental consequences for stability and toxicity. Thus, surface passivation of 8 nm cobalt ferrite NMs, besides the formation of an iron-rich surface layer, was observed to improve the crystal quality while altering the Fe/Co cation distribution and the NM dissolution rate profile (Soler 2007). Magnetic data revealed that the saturation magnetization increased for surface-passivated NMs compared to the non-passivated ones, though coercivity decreased after passivation. These two phenomena occurred due to changes in the cation distribution among the available tetrahedral and octahedral sites (Soler 2007). Another important outcome from this study is that all of the aged magnetic fluid NM samples deviated from the precursor stoichiometry, thus revealing a discrepancy in the dissolution of cobalt ferrite NMs, which influenced the lattice parameter value (Soler 2007). This highlights the fact that *change of one parameter may inadvertently affect another (or several other) parameter(s)* with direct consequences for quantitative property-activity relationships.

NM composition is the main determinant of whether a NM will dissolve or not, which is linked to the elements' solubility in water. However, as shown in Table 2, particle size and size distribution, which are linked to particle surface area, also influence the rate of dissolution, which typically occurs from the surface. Crystal

Table 2 Contributions of various physico-chemical properties (from Table 1) to the different toxicity mechanisms described here

Measured parameters	Dissolution	NM interactions	NM (surface) specific effects	Trojan Horse
Size/size distribution	✓✓	✓	✓	✓✓
Surface area	✓✓	✓✓	✓✓	✓✓
Purity (particle/dispersant)	~	✓	–	–
Photochemical activity	✓	✓	✓	–
Surface charge/chemistry	✓	✓✓	✓	✓✓
Hydrophobicity	~	✓✓	–	✓✓
Redox activity	✓	–	✓	–
Shape	✓✓	✓	✓✓	✓
Crystal structure	✓✓	✓✓	✓✓	✓✓
Porosity/surface defects	✓	✓	✓✓	✓

Two ticks indicate strong contribution, one tick indicates some contribution, ~ indicates not clear as yet while – indicates likely no significant contribution. Note that these are opinions rather that quantitative values. Measuring the relative contributions quantitatively is challenging and has yet to be achieved

structure and phase also play a role, with faces having coordination numbers {1 1 1} and {1 1 0} dissolving faster than others such as the {1 0 0} face of nanocrystals (Liu 2008; Misra 2012). Shape is also an important parameter, again linked to surface area, but also as narrow areas will dissolve faster that thicker ones. To a lesser degree (although this has not been quantified but is rather an opinion) porosity, again linked to surface area, as well as photochemical and redox activity will drive dissolution, as most cases of nanoparticle (NP) dissolution under environmental conditions are driven by oxidative processes (Ho 2010).

2.2 NM Interactions

2.2.1 Cationic Surface Charge (as Determined by Zeta Potential) Linked to Membrane Damage

The toxic mechanism of a 60-nm cationic (amino-functionalized) polystyrene NM (PS-NH_2) in bacterial cells was explored using a genome-wide collection of bacterial single-gene deletion mutants (Ivask 2012). Over 4000 single nonessential mutants of *Escherichia coli* were screened for the growth phenotype of each strain in the presence and absence of PS-NH_2. The largest number of genes contributing to bacterial sensitivity for PS-NH_2 nanospheres was associated with the formation and functioning of the bacterial cell membrane, followed by defects in lipopolysaccharide and ubiquinone biosynthesis, flagellar formation, and DNA repair. The authors assumed that the proper formation, stability, and functionality of the bacterial cell wall are necessary for the bacteria's ability to compete against cationic NM-induced stress (Ivask 2012). ROS production was also shown to be a crucial pathway of toxicity for PS-NH_2; importantly, it was observed that there is at least one mutant for which there is an additive effect between ROS sensitivity and disruption of membrane integrity. This finding indicates that these two toxicity mechanisms are independent (i.e., disruption of membrane integrity is not necessarily due to ROS production by the NM) (Ivask 2012).

As indicated in Table 2, surface charge thus plays an important role in determining NM interactions with biological and environmental macromolecules, including those incorporated into key biological membranes. Here, hydrophobicity and redox activity will also play a key role in moderating the observed toxicity, with hydrophobicity helping to anchor the NMs close to membranes, and redox activity providing a supply of ROS to amplify the damage from the NMs.

2.2.2 Point of Zero Charge (PZC) and Critical Coagulation Concentration (CCC)

A useful alternative to zeta potential (ζ-potential) measurements [which are very often poorly presented and misinterpreted in the literature, as zeta potential depends

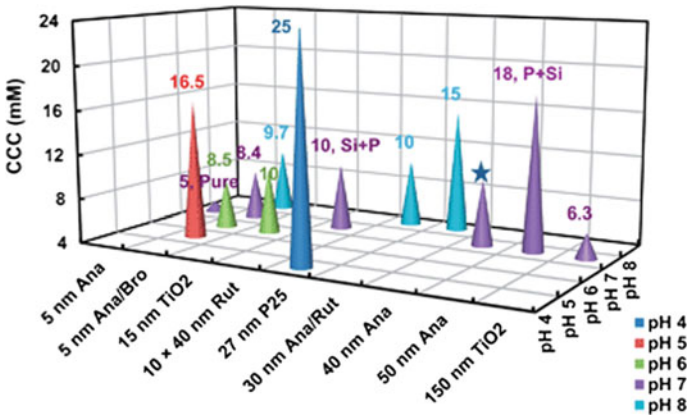

Fig. 3 Comparison of CCC for the TiO_2 NMs with different crystallinity, morphology, and composition at various pH values as reported in the literature (from Liu 2013b and references therein). The CCC values at acidic pH (e.g., pH 5) were generally higher than at neutral pH (e.g., pH 7), which is close to the PZC. The CCC for 10 × 40 nm rutile (10 mM) and 50 nm anatase (18 mM) were higher compared with the 5 nm anatase (5 mM), due to the detected impurities of Si and P and consequently more negative surface charge at pH 7. Further analysis on the material properties of the other TiO_2 is not feasible, due to the insufficient information on the composition of the pristine TiO_2. The *star symbol* stands for the estimated value of CCC, due to the unavailability of the aggregation kinetics data. *Ana* anatase, *Rut* rutile, *Bro* brookite. From Liu (2013b)

on ionic strength, pH and agglomeration/aggregation (Lowry 2016)] is to take into account the context-dependent parameters, such as the point of zero charge (PZC) and the critical coagulation concentration (CCC), since these properties require experimentation under titrating conditions, therefore having less room for dangerous misunderstandings.

An elegant approach to evaluate which physico-chemical properties of TiO_2 NMs and carbon nanotubes determine their environmental stability and transport was recently proposed, although full implementation was prevented by the lack of relevant data under realistic exposure conditions (Liu 2013b). This study showed a high correlation among impurities (including Si and P) resulting from the synthesis route and the PZC, which was in turn correlated with the CCC (Fig. 3) and some implications for transport were discussed. It was suggested that in order to diminish the environmental risks of TiO_2 NMs alternative procedure or chemicals that are Si- and P-free are preferable to use during synthesis (Liu 2013b).

However, in the environment, the adsorption of natural organic matter (NOM) can significantly influence the surface properties and behaviour of TiO_2 NMs (from Liu 2013a and references therein). Thus, further studies are needed regarding the interactions between NOM and TiO_2 of varying properties, as well as to determine whether the property of adsorbed NOM or TiO_2 mainly controls the stability and transport in the natural environment (Liu 2013a).

Other physico-chemical properties strongly linked with NM stability and thus exposure dose and resulting toxicity are photochemical activity, in so much as this can alter the surface composition and thus the PZC and CCC, and likely also crystal structure.

2.2.3 Biological Surface Adsorption Index (BSAI)

A biological surface adsorption index (BSAI) has been proposed as a way to describe the interactions between NMs and biomolecules by estimating the competitive adsorption of a set of small molecule probes onto the NMs (Fig. 4). This is achieved by mimicking the molecular interactions of the NM with the protein residues (Xia 2010). The adsorption of NMs is assumed to depend on Coulomb forces (charged particles), London dispersion (hydrophobic interactions), hydrogen-bond (HB) interactions, dipolarity/polarizability, and lone-pair electrons. Adsorption coefficients of the probe compounds were measured and then were used to construct a set of nanodescriptors representing the contributions and relative strengths of each molecular interaction. The method successfully predicted the

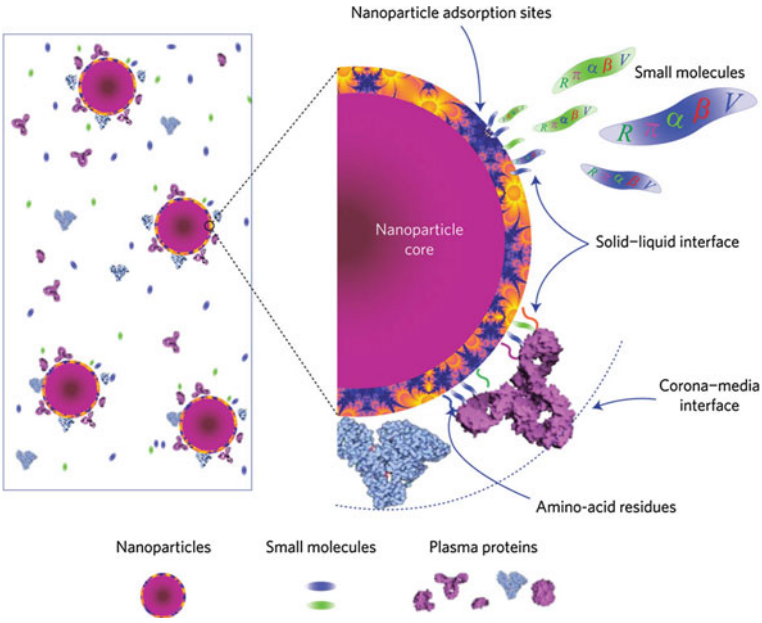

Fig. 4 *Left* in a physiological environment, NMs are exposed to various proteins and small molecules. *Right* the competitive adsorption of small molecules (*upper*) and the residues of proteins (*lower*) on an NM. The *orange ring* on the NM with blue irregular shapes represents the adsorption sites that are not uniformly distributed on the surface. Small molecules with known molecular descriptors [R, π, α, β, V] can be used as probes to measure the molecular interaction strengths of the NMs with small molecules and biomolecules. From Xia (2010)

adsorption of various small molecules onto carbon nanotubes, and the nanodescriptors were also calculated for 12 other NMs (Xia 2010).

The adsorption coefficients of the probe compounds on a given NM (e.g., multi-walled carbon nanotubes—MWCNTs) were measured using a solid-phase microextraction (SPME)–gas chromatography mass spectrometry (GC–MS) method. The correlation of logk with the solute descriptors was established after multiple linear regression analysis of the [logk, R, π, α, β, V] matrix, where logk is the adsorption coefficients of a probe compound (that binds to the MWCNT) and [R, π, α, β and V] are solvation descriptors of the probe compounds—Coulomb forces, London dispersion, hydrogen-bond acidity and basicity, polarizability and lone-pair electrons (Xia 2010). Thus, the BSAI approach provides rational interpretations for the molecular interactions, and also yields five physico-chemical parameters, which characterize the relative strengths of the molecular interactions of the NMs (Xia 2010).

The BSAI nanodescriptors can be related to membrane interaction and biodistribution properties (e.g., absorption rate, distribution coefficient and extent of cellular uptake) of the NM to develop physiologically based pharmacokinetic models, and also for quantitative risk assessment and safety evaluation of NMs (Xia 2010).

Other key physico-chemical parameters affecting biomolecule binding, and thus conferring a biological identity and influencing NM toxicity, include hydrophobicity, surface area and surface curvature (linked to NM size), and crystal structure, as indicated in Table 2. Different NM crystal faces have different energies, resulting in different binding affinities for biomolecules (Lynch et al. 2014a; Sund 2011).

2.2.4 *NM-Binding Induced Changes in Protein Conformation May Lead to Receptor Activation*

A series of studies using negatively charged poly(acrylic acid)-conjugated gold NMs of various sizes has shown that particle size may affect protein structural changes resulting from binding, which can then induce different modes of interaction between NMs and cells or tissues (Deng 2011, 2013). Activation of the integrin receptor (Mac-1) by 5 nm poly(acrylic acid)-conjugated gold NMs was found to occur due to conformational changes of the bound fibrinogen, leading to increased nuclear factor NF-κB signalling, which in turn resulted in the release of inflammatory cytokines (Deng 2011). However, larger [20 nm poly(acrylic acid)-conjugated] gold NMs, which also bound fibrinogen, did not induce this effect. This is a *clear demonstration of a NM-protein binding-induced signalling pathway and suggests an alternative mechanism to the more commonly described role of oxidative stress in the inflammatory response to NMs.*

A follow-on study to estimate the effect of binding to gold NMs of different size (5–20 nm) with different surface charge on fibrinogen conformation showed that fibrinogen bound with high affinity to both (positively and negatively charged) NM (Deng 2013). However, binding kinetics and protease digestion suggested that each

NM adopted a different binding orientation, and verified that only the negatively charged NMs induced cytokine release from THP-1 cells (Deng 2011). It was concluded that "*since common proteins can bind to different NMs with quite different biological outcomes, knowledge of the composition of the protein corona is not sufficient to predict biological effects of NMs, and conformational and orientational information is also required*".

Other NM factors known to influence protein unfolding and formation of so-called cryptic epitopes which can lead to novel toxicities (Lynch 2007), include hydrophobicity, surface curvature [linked to NM size (Klein 2007)] and porosity or surface defects (Clemments 2015).

2.3 NM (Surface) Specific Effects

2.3.1 Surface Defects, Including Those Induced by Surface Oxidation

A study of the effect of nanosize Ag spheres, plates, and wires on a fish gill epithelial cell line (RT-W1) and on zebrafish embryos showed significantly increased toxicity from the Ag nanoplates compared to the other particle shapes (George 2012). Features, such as Ag ion shedding and bioavailability failed to thoroughly explain the enhanced toxicity of the nanoplates. High-resolution transmission electron microscopy showed a high level of crystal defects (stacking faults and point defects) on the nanoplate surfaces. A noticeable reduction of toxicity in RT-W1 cells and zebrafish embryos was observed upon surface coating with cysteine to passivate the surface defects (George 2012).

Graphene oxide (GO) is considered as being biocompatible, but until recently there has been a limited amount of data to verify this. Currently, four general top-down routes for GO production use different acids to oxidise the surface and offer hydrophilicity. The cytotoxicity of GOs (prepared by the four oxidative treatments above) was measured by means of the mitochondrial activity in adherent lung epithelial cells (A549), using commercially available viability assays (MTT and WST-8) (Chng 2013). All four GO NMs yielded strong dose-dependent cytotoxic responses after 24 h exposure, and a relation between the oxygen content/functional groups of GOs with their toxicological response against the A549 cells was observed: The various oxidative approaches produced GOs with different properties due to varying C/O ratios and proportions of the types of oxygen-containing groups (e.g., carbonyl group) (Chng 2013). *This is the first study, which demonstrates how the oxidative routes employed to prepare GOs (also other carbon-based NMs) may profoundly affect their toxicity.*

Another article demonstrating that the selected method to vary the NM physico-chemical features can itself induce other unwanted effects is that of Bussy et al. (2012), where the impact of carbon nanotube length on toxicity was investigated (Bussy 2012). A broad study was designed to compare the effects of two samples of MWCNT (synthesized following a similar production process, i.e.,

aerosol-assisted CVD) on murine macrophages; a soft ultrasonic treatment in water was used to change the length of one of the MWCNTs (Bussy 2012). It was shown that altering the length of MWCNT leads to associated structural (i.e., defects) and chemical (i.e., oxidation) changes that affect both surface and residual catalyst iron NM content of the CNT. The structural defects and oxidation (induced by the length reduction process) were shown to be at least as responsible as the length reduction itself for the increased pro-inflammatory and pro-oxidative response observed with short (oxidized) MWCNT compared to long (pristine) MWCNT (Bussy 2012). This further demonstrates the problem of the inter-dependence of various physico-chemical properties and the *significant challenges inherent in the development of systematically varied libraries of NMs as the basis for mechanistic studies*. However, designing libraries with this knowledge of predicted physico-chemical interdependencies in place will allow this information to be included into the physico-chemical testing strategy and into the structure-property relationships under development.

2.3.2 Bandgap as a Proxy for Oxidative Stress

Oxide semiconductors can serve as channels for electron transfer between aqueous reactants. The occurrence of these transfers depends on similarities in the energetic states of the NMs and ambient redox-active aqueous substances (Zhang 2012b). Burello and Worth proposed a theoretical scheme where the relationship between the cellular redox potential to metal oxide (MOx) band gap clarifies the observed oxidative stress and toxicity generation by some of these materials (Burello 2011). According to this band gap hypothesis, it is possible to predict the oxidative stress potential of MOx NMs by comparing the E_v (valence band) and E_c (conduction band) levels to the cellular redox potential (Burello 2011).

Using a panel of 24 MOx NMs (George et al. 2012) showed that with the use of conduction band energy levels (band gap), it is possible to describe their toxicological potential at cellular and whole organism levels. Among the NMs, the overlap of conduction band energy (E_c) levels with the cellular redox potential (−4.12 to −4.84 eV) was strongly associated with the ability of Co_3O_4, Cr_2O_3, Ni_2O_3, Mn_2O_3 and CoO NMs to induce oxygen radicals, oxidative stress, and inflammation (George 2012). Although CuO and ZnO produced oxidative stress and acute pulmonary inflammation, which is not predicted by E_c levels, the adverse biological effects of these NMs are explained by their solubility, as demonstrated by ICP-MS experiments (George 2012). These results indicated that the toxicity of a large series of MOx NMs can be predicted in the lung based on semiconductor properties and an integrated in vitro/in vivo hazard ranking model based on oxidative stress. It is not yet clear whether there are additional factors that contribute to band-gap in addition to crystal structure and composition, although for silicon wires bond angles and bond strain cause a transition from direct to indirect band gap behaviour and the properties can be tailored through surface chemistry (Brus 1994). This could be an area for future nanosafety research, focussing on, for

example, the role of porosity, defects, doping or anion exchange on energy transfer within nanocrystals.

2.4 NM Trojan Horse Effects—Increased Local Concentrations of (Dissolved) Species

In medicine, the Trojan horse effect is defined as "Any disastrous result of an anticipated gain; or, the masking of a dangerous agent within an innocent garb".[1] There are numerous cases where NMs act as Trojan horses, both when the NM alone releases high concentrations of ionic species in sites that they would not normally reach such high concentrations (Park 2010; Studer 2010), and when the NM carries another compound along, thus accessing an otherwise inaccessible location (Baun 2008). Both types of the Trojan horse effect are based on the size properties and biomolecule adsorption of NMs, which enable them to participate in the active receptor-mediated transport processes of cells and organisms that are often less accessible to ionic or molecular species, which are typically internalised based on passive diffusion (Salvati 2011).

Silver NMs (distributed in foetal bovine serum, average size: 68.9 nm, concentrations: 0.2, 0.4, 0.8, and 1.6 ppm, exposure time: 24, 48, 72, and 96 h) appeared cytotoxic to cultured RAW264.7 cells by increasing sub G1 fraction, which denotes cellular apoptosis (Park 2010). Silver NMs were found in the cytosol of activated cells, whereas were absent in the dead cells, thus suggesting their dissolution and release of ions and cytotoxicity by a Trojan-horse type mechanism (Park 2010). Studer et al. (2010) studied the toxicities of copper oxide and carbon coated copper metal NMs at constant copper exposure dose, and observed noticeably different responses from the two NM forms: while copper oxide was highly cytotoxic, carbon-coated copper NMs were much less cytotoxic and more tolerated, which corresponded with the two material's intra- and extracellular solubility in model buffers (Studer 2010). Thus, the differences in toxicity correlated with different copper release in line with a Trojan horse-type scenario.

C_{60}-NMs (Buckminster fullerenes) are known to function as carriers of contaminants in aqueous systems. This has been verified in a series of toxicity tests with algae (*Pseudokirchneriella subcapitata*) and crustaceans (*Daphnia magna*) with four common environmental contaminants (atrazine, methyl parathion, pentachlorophenol (PCP), and phenanthrene) as model compounds with different physico-chemical properties and toxic modes of action (Baun 2008). In algal tests, C_{60}-aggregates increased the toxicity of phenanthrene by 60% and decreased the toxicity of PCP about twofold. Addition of C_{60}-aggregates increased the toxicity of phenanthrene ten fold when results were expressed as water phase concentrations. Metals, such as Cd bound to NM (e.g., titania) surface, show increased bioavailability in fish (carp) (Shaw

[1] http://medical-dictionary.thefreedictionary.com/Trojan+Horse+Effect.

2008). Since many NMs are negatively charged, they act as suitable carriers for cationic metals. The data mentioned above underline that *both inherent toxicity of manufactured NMs, and interactions with other compounds and characterisation of NMs in aqueous suspension are crucial data for risk assessment of NMs.*

Table 2 also highlighted the range of physiochemical parameters that can play a role in determining pollutant binding to NMs, as a prerequisite for Trojan horse effects resulting from the pollutant gaining a new access route carried on the NM. This also shows that the same NM physico-chemical parameter may contribute to multiple modes of action, which may occur simultaneously.

3 Systematic NM Libraries Reported in the Literature

To associate particular physico-chemical properties of an NM with its toxicity, it is imperative to establish combinatorial libraries, constructed in a way that systematic variation of important physico-chemical properties (probably related to toxicity) can occur (Xia 2012). Property variations may include NM size, shape, surface area, band gap, porosity, crystallinity, charge, solubility, and surface functionalization, as shown in Fig. 5.

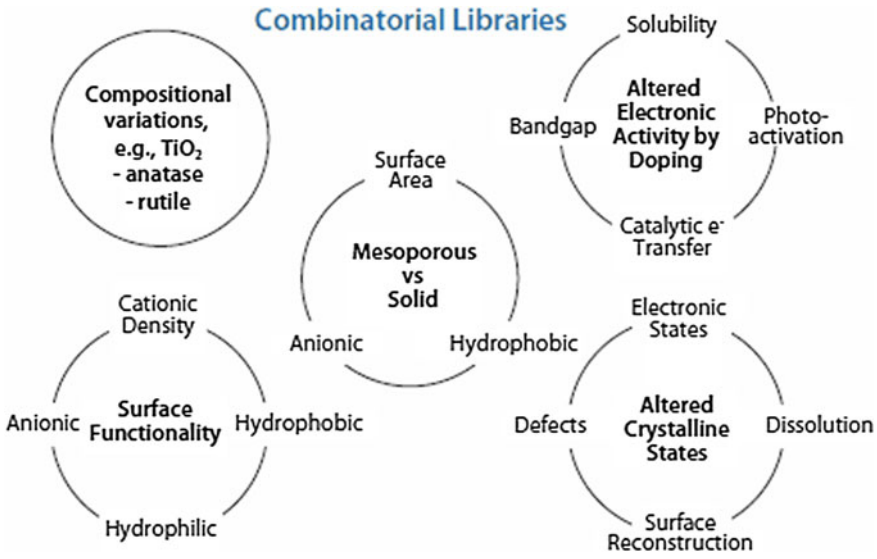

Fig. 5 Examples of combinatorial NM libraries. Combinatorial libraries are constructed by synthesizing one of the compositional NMs to vary physico-chemical properties, which may be involved in toxicity. Property variations apply to NM size, shape, charge, porosity, hydrophilicity, hydrophobicity, crystallinity, band gap, photoactivation, solubility, and surface area. A single property change may also affect other properties, thus rigorous re-characterization is required. From Xia (2012)

Here, we offer an overview of the types of NM libraries that have been developed in academic groups to date, although these are not available commercially, and they have typically varied only one or two materials, thus preventing safe generalisations. Important attempts to develop QNARs based on these libraries are also presented. So far, two tools to address the need for constructing validated QNARs have been developed and are disseminated as ready-to-use applications for anyone interested in NMs risk assessment. These tools aim to investigate the NMs' diverse effects by estimating the impact of different surface modifiers on cellular uptake and by exploring the dependency between various physico-chemical descriptors of iron oxide and toxicity. These two approaches may facilitate ongoing research on the identification of the crucial descriptors for the virtual screening of NMs diverse effects.

One of the few organized datasets of NMs that has been presented in the literature contains the cellular uptake of 109 NMs in pancreatic cancer cells (PaCa2). Each NM within this dataset involves the same metal core (iron oxide/NH_2 cores) but different surface modifiers, which are small organic molecules conjugated to the NM surface (Weissleder 2005). For the development of our first tool, we have constructed and validated a QNSAR model for the prediction of the cellular uptake in pancreatic cancer cells based on this dataset. The in silico workflow is available online through the Enalos InSilicoNano platform (http://enalos.insilicotox.com/QNAR_PaCa2/), which is a web service based solely on open source and freely available software that was developed to make our model available to any one aiming at acquiring knowledge on potential biological effects in the decision making framework (Fig. 6). To test the usefulness of the web service, the entire PubChem database was exploited to select compounds similar to a known active structure. Next, the Enalos InSilicoNano platform was used to identify novel potent NMs from a prioritized list of compounds (Melagraki 2014).

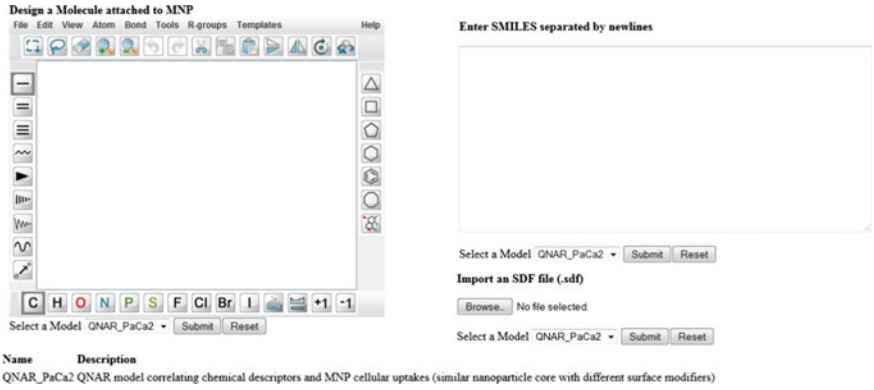

Fig. 6 Screenshot of the Enalos Platform input page for the prediction of NMs uptake in PaCa2 cells

A second online tool for the computational screening of iron oxide NMs was also developed to complement our previously reported efforts to extract valuable information from available datasets and to develop user friendly applications for the risk assessment of NMs. For this purpose, a predictive classification model was developed for the toxicological evaluation of 44 iron oxide NMs with different core, coating and surface modifications based on several different properties, such as size, relaxivities, zeta potential and type of coating (Shaw 2008).

The model was fully validated through several validation tests and was released online via the Enalos InSilicoNano Platform (http://enalos.insilicotox.com/QNAR_IronOxide_Toxicity/). This web service allows a user to insert specific properties (Fig. 7) and subsequently to obtain a toxicity prediction (and an indication of the reliability of the prediction) based on the domain of applicability (Melagraki 2015).

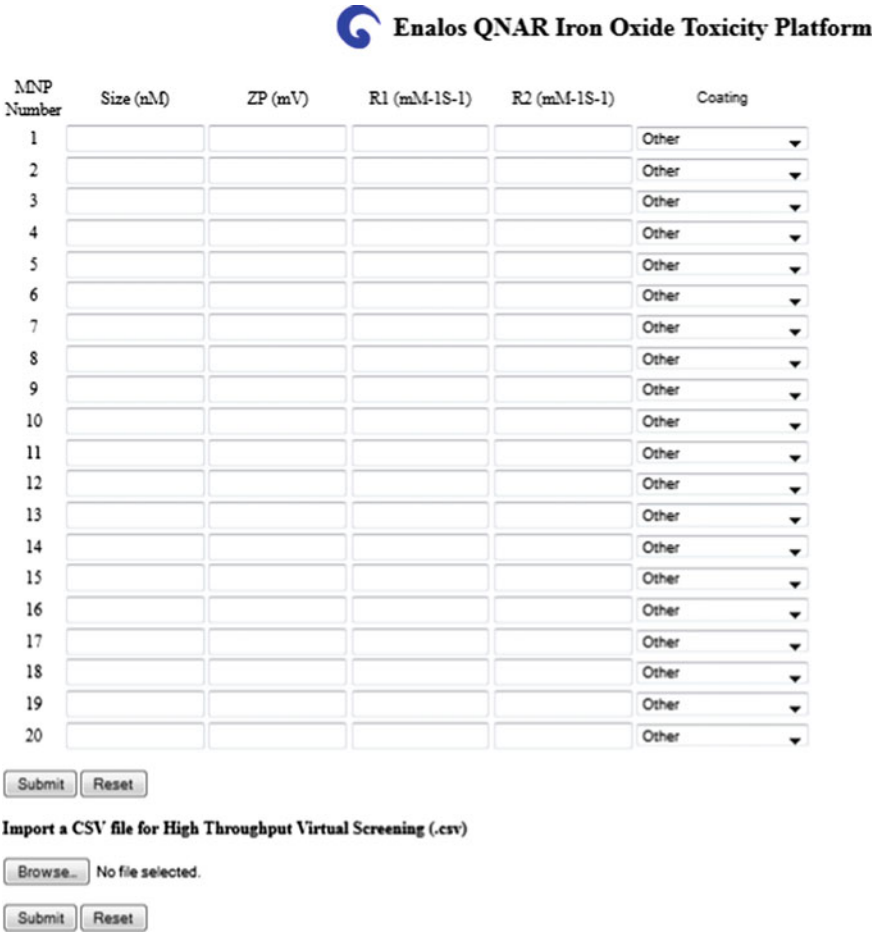

Fig. 7 Screen shot of Enalos QNAR iron oxide toxicity platform input page

These freely available web services are the first efforts to establish an online tool that the wider scientific community can easily apply in the computer-aided NM design and may be a means to reliably predict the activity of novel nano-structures. The user friendly environment enables different datasets to be directly imported based on the particular requirements of the user. Both web services offered via the Enalos InSilicoNano platform aim to provide significant aid within a virtual screening framework, for the design of novel NMs or their prioritization based on predicted diverse effects.

3.1 Gold Nanoparticle Libraries

Gold nanoparticles were selected by a group at the university of Oregon to represent an ideal platform for the systematic evaluation of the effect of various physico-chemical properties (including core size, charge, and surface chemistry) on biological responses to NM exposure (Harper 2011). A matrix of nine structurally diverse, precision-engineered Au NMs of high purity and known composition was constructed. This included three core sizes and four unique surface coatings that contain positively and negatively charged head groups, as shown in Fig. 8.

Testing the different combinations of core sizes and ligand shells enabled evaluation of the importance of small changes in core size and ligand composition independently. Zebrafish embryo mortality, malformations, uptake, and elimination of Au NMs depended on the above parameters, thus highlighting the need for very careful experimental design and NM characterization (Harper 2011).

Besides the great control over particle size and the simple functionalization through surface modification (Fig. 9), gold NMs are excellent systems for further development of NMs libraries, due to the recent developments in controlling the shape of the nanocrystals (Sau 2009). The size, shape, and structural control of the nanocrystals is achieved through handling of the kinetic and thermodynamic parameters of the systems with the aid of additives, light and thermal energy, as well as their combinations (Sau 2009 and references therein). The formation of diverse shapes most likely arises from the relationship between the faceting tendency of the stabilizing agent and the growth kinetics (rate of supply of Au^0 to the crystal planes) (Ahmadi 1996). Sau et al. presented a seed-mediated growth method to regulate the morphology and dimensions of gold nanocrystals by manipulating the experimental parameters in aqueous medium at room temperature (Sau 2009). This chemical procedure generated several architectures with rod-, rectangle-, triangle-, hexagon-, cube-, and star likes structures and branched (i.e., bi-, tri-, tetra-, and multipod) Au nanocrystals of varied dimensions in high yield, in the presence of a single surfactant (cetyltrimethylammonium bromide, Fig. 8) (Sau 2004). Although this surfactant is not typically used in toxicology studies, this work makes evident that shape maybe changed in a manner such that all shapes result from identical starting structures. This observation is important because it suggests that only the shape changes from one material to another, while other parameters (e.g.,

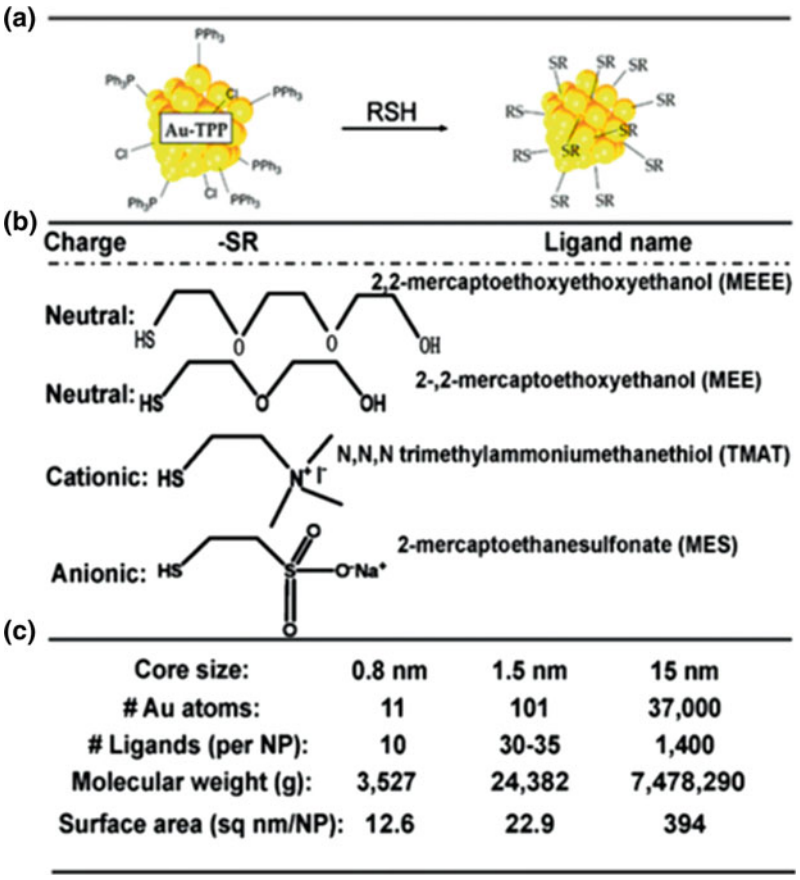

Fig. 8 Gold NM synthesis, structure, and properties. **a** Synthesis reaction of functionalized gold NMs from gold triphenylphosphine (AuTTP) NM building blocks. **b** Name, charge, and structure are provided for each ligand tested. **c** Properties with implications for dose metrics for the different NM core sizes are also given. From Harper (2011)

defects, faceting face etc.) are also obviously affected. Moreover, this approach would allow the *experimental evaluation of differences in biomolecule binding, diffusion and interaction with receptors* etc. *based on NM shape in a systematic manner. This may constitute the basis for further improvement and validation of models and QSARs*. For example, molecular dynamics (MD) simulations have shown that the efficacy of passive endocytosis is higher for spherocylindrical particles compared to spheres and that endocytosis is abolished for sharp-edge particles (Vácha 2011).

Walkey et al. have recently presented the synthesis and experimental evaluation of a chemically diverse set of 105 gold NMs with various surface modifiers (Walkey 2014). The authors considered three different core sizes, namely 15, 30

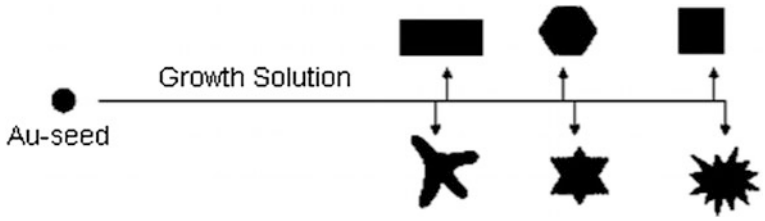

Fig. 9 Schematic illustration of the variation of gold NM morphology and dimensions (shape and structure) by manipulation of the experimental parameters in aqueous solution at room temperature. From Sau (2004)

and 60 nm, and employed 67 organic surface modifiers, which included small molecules, polymers, peptides, surfactants and lipids that can be identified as "neutral", "anionic" and "cationic" according to their structural and charge properties at physiological pH. Different parameters for each NM were measured before and after exposure in blood serum stimulating the biomolecular environment during in vitro cell culture experiments. In total, 21 physico-chemical parameters before and after exposure were calculated and 785 distinct serum proteins were recognized on the NMs. Furthermore, all NMs were evaluated regarding their association with A549 human lung epithelial carcinoma cells (Albanese 2014).

3.2 Metal Oxide Nanoparticle Libraries

The Centre for Environmental Implications of Nanoscience and Nanotechnologies at UCLA have developed a compositional library of 24 different metal oxide NMs (whose compositions, size distribution and zeta potential are shown in Table 3), which was constructed to explore the correlation of NM electronic properties and their toxicity results (Lin et al. 2013). Most of the NMs were directly purchased, and others (CuO, Co_3O_4, Fe_3O_4, Sb_2O_3, TiO_2, WO_3, and ZnO) were synthesized in-house by flame spray pyrolysis (Teoh 2010). The results of Table 3 suggested that the hydrodynamic size of these NMs in Holtfreter's medium (pH 7.0) ranges from 200 to 500 nm, with only a few materials (Al_2O_3, Fe_3O_4, Ni_2O_3, SnO_2, Y_2O_3, Yb_2O_3) reaching 500 nm. The ζ-potentials of all NMs were negative (−20 to −30 mV) due to alginate coating.

Using the above NM library, Lin et al. (2013) established a predictive toxicological paradigm (that of metal oxide dissolution and ligation of the zebrafish hatching enzyme 1 (ZHE1) enzyme centre by specific metal ions), which can be used for the safety evaluation of dissolved metal oxide NMs in aqueous media. The excellent correlation between ZHE1 inactivation and hatching interference in intact embryos rationalized the molecular mechanism of hatching interference exerted by CuO, ZnO, Cr_2O_3 and NiO NMs (Lin et al. 2013). The authors concluded that shedding of metal ions by dissolvable metal oxide NMs interferes with recombinant

Table 3 Physico-chemical features of 24 metal oxides in the UCLA library

Number	MOx	Primary size (nm)[a]	Hydrodynamic size (nm)[b]	Zeta-potential (mV)[c]
1	Al_2O_3	14.7 ± 5.2	524.8 ± 32.8	−24.0 ± 0.5
2	CeO_2	12.8 ± 3.4	321.3 ± 8.6	−28.9 ± 3.3
3	CoO	18.3 ± 6.8	378.3 ± 16.4	−25.5 ± 1.3
4	Co_3O_4	10.0 ± 2.4	247.6 ± 16.9	−29.0 ± 2.2
5	Cr_2O_3	71.8 ± 16.2	478.5 ± 7.2	−26.2 ± 3.1
6	CuO	193.0 ± 90.0	289.5 ± 31.0	−26.9 ± 0.8
7	Fe_2O_3	12.3 ± 2.9	385.2 ± 6.3	−24.1 ± 2.0
8	Fe_3O_4	12.0 ± 3.2	831.7 ± 41.8	−27.0 ± 2.3
9	Gd_2O_3	43.8 ± 15.8	726.7 ± 54.8	−34.7 ± 0.7
10	HfO_2	28.4 ± 7.3	349.9 ± 5.2	−24.3 ± 2.1
11	In_2O_3	59.6 ± 19.0	303.2 ± 5.2	−35.5 ± 2.4
12	La_2O_3	24.6 ± 5.3	471.2 ± 20.9	−27.8 ± 0.6
13	Mn_2O_3	51.5 ± 7.3	525.9 ± 7.8	−30.9 ± 0.4
14	NiO	13.1 ± 5.9	277.5 ± 23.0	−23.1 ± 2.0
15	Ni_2O_3	140.6 ± 52.5	665.8 ± 46.4	−24.4 ± 2.2
16	Sb_2O_3	11.8 ± 3.3	459.9 ± 22.7	−25.8 ± 0.9
17	SiO_2	13.5 ± 4.2	374.9 ± 29.0	−16.8 ± 2.0
18	SnO_2	62.4 ± 13.2	635.0 ± 52.0	−26.4 ± 0.3
19	TiO_2	12.6 ± 4.3	497.0 ± 17.1	−31.5 ± 1.4
20	WO_2	16.6 ± 4.3	511.9 ± 19.4	−23.3 ± 1.1
21	Y_2O_3	32.7 ± 8.1	594.5 ± 33.0	−27.6 ± 0.4
22	Yb_2O_3	61.7 ± 11.3	682.6 ± 56.2	−29.7 ± 0.5
23	ZnO	22.6 ± 5.1	379.0 ± 11.0	−27.0 ± 1.1
24	ZrO_2	40.1 ± 12.6	384.4 ± 25.0	−19.7 ± 3.6

From Lin et al. (2013)

[a]Primary size of particles in their dry state was obtained by transmission electron microscopy (JEOL, 1200 EX)

[b]Hydrodynamic size was determined by high throughput dynamic light scattering (HT-DLS, Dynapro Plate Reader, Wyatt Tech)

[c]Particle ζ-potential was measured using ZetaPALS (Brookhaven Instruments, Holtsville, NY). Introduction of the NPs in Holtfreter's medium (pH 7.0) did not significantly change the medium pH in spite of the dissolution of metal oxide NPs

ZHE1 activity. Consequently, it was anticipated that CuO, ZnO, Cr_2O_3 and NiO NMs should interfere in embryo hatching (Lin et al. 2013).

A classification-based cytotoxicity nanostructure-activity relationship (nano-SAR) with excellent classification accuracy was developed based on four descriptors: atomization energy of the metal oxide, period of the NM metal, NM primary size, and NM volume fraction (in solution). Based on a set of 9 metal oxide NMs to which transformed bronchial epithelial cells (BEAS-2B) were exposed over a range of concentrations and exposure times up to 24 h, the best-performing model had a 100% classification accuracy in both internal and external validation (Liu 2011).

Additional applications of this NM library include the evaluation of a possible connection between conduction band energy levels and toxicity, specifically oxidative stress and acute pulmonary inflammation (Zhang 2012b). The authors employed the same set of NMs from Table 3 to prove that the overlap of conduction band energy (E_c) levels with the cellular redox potential (−4.12 to −4.84 eV) was highly correlated to the ability of Co_3O_4, Mn_2O_3, Cr_2O_3, Ni_2O_3 and CoO NMs to induce oxygen radicals, oxidative stress, and inflammation (Zhang 2012b).

Recently, the UCLA Centre have also used the flame spray pyrolysis (FSP) technique to construct NM libraries where metal oxides are doped with Fe to diminish their solubility or toxicity (e.g., pure or Fe-doped ZnO or TiO_2 NMs) (Pokhrel 2012). It was demonstrated that FSP is a flexible method for the effective design of a homologous library (i.e., a library based on a parent oxide, which is doped with various amounts of dopant) and may also serve as a tool for exploring the properties of the resulting compounds (Pokhrel 2012).

Another NM library of 17 metal oxides (size range: 15–90 nm) was established by Puzyn et al. (2011). Experimental and computational results related to the toxicity of the NMs in terms of predicted EC_{50} values (calculated using a single descriptor, ΔH_{Me+} describing ionization enthalpy of the detached metal atoms) are shown in Table 4 (Puzyn et al. 2011). Since particle size does not significantly affect toxicity in the above size range, the chosen descriptors essentially represent reactivity-related electronic properties. The NMs, which were used in the training set to develop the QSAR equation are denoted by *T* (Table 4), and the NMs in the validation sets by V_1 and V_2. The model reliably predicted the toxicity of all compounds under study (Puzyn et al. 2011).

3.3 Silica Nanoparticle Library

A silica NM library consisting of 12 variants of amorphous Stöber silica, mesoporous silica, amorphous fumed silica, silicalite and α-quartz was constructed to investigate the crystallinity and surface effects of silica NMs (Zhang 2012a). Particular physico-chemical properties, such as size, size distribution and zeta potential in water and two different media (containing protein or serum) of the different NMs are presented in Table 5. Initial studies indicated that fumed silica is the most toxic among the silicas in the library (Zhang 2012a). The toxicity can be reduced by heating and re-imposed by hydration. The changes are most likely related to the number of surface silanol groups and strained three-member Si rings (Zhang 2012a).

Table 4 Experimental and predicted features of metal oxides used in the Puzyn study

Metal oxide	Descriptor ΔH_{Me+} (kcal mol^{-1})	Leverage value, *h*	Observed log 1/EC_{50} (mol l^{-1})	Predicted log 1/EC_{50} (mol l^{-1})	Residuals	Set
ZnO	662.44	0.33	3.45	3.30	0.15	*T*
CuO	706.25	0.29	3.20	3.24	–0.04	*T*
V_2O_3	1,097.73	0.11	3.14	2.74	0.40	V_1
Y_2O_3	837.15	0.21	2.87	3.08	–0.21	*T*
Bi_2O_3	1,137.40	0.10	2.82	2.69	0.13	*T*
In_2O_3	1,271.13	0.10	2.81	2.52	0.29	*T*
Sb_2O_3	1,233.06	0.10	2.64	2.57	0.07	V_1
Al_2O_3	1,187.83	0.10	2.49	2.63	–0.14	*T*
Fe_2O_3	1,408.29	0.13	2.29	2.35	–0.06	*T*
SiO_2	1,686.38	0.26	2.20	1.99	0.21	*T*
ZrO_2	1,357.66	0.11	2.15	2.41	–0.26	V_1
SnO_2	1,717.32	0.28	2.01	1.95	0.06	*T*
TiO_2	1,575.73	0.19	1.74	2.13	–0.39	*T*
CoO	601.80	0.38	3.51	3.38	0.13	V_2
NiO	596.70	0.39	3.45	3.38	0.07	V_2
Cr_2O_3	1,268.70	0.10	2.51	2.52	–0.01	V_2
La_2O_3	1,017.22	0.13	2.87	2.85	0.02	V_2

From Puzyn et al. (2011)
The leverage value h (acceptable if not higher than 0.6) indicates deviations of the structure of the compound from those used for the QSAR development

3.4 Single-Wall Carbon Nanotube Library

A three-particle (HiPco-D, SG65-D, and P2-D), single-walled carbon nanotube (SWCNT) library was created to explore the impact of hydrophobicity, metal impurity, and dispersion state on NM toxicity (Chowdhury et al. 2012). In Table 6, the physico-chemical features and the metal contaminants are presented. Using these three SWCNTs, Chowdhury et al. (2012) initiated a study to correlate their transport with the various synthetic methods and residual catalyst contents in order to elucidate their effect on the nanotubes (Chowdhury et al. 2012). After purification, the residual metal catalyst between the SWCNTs follows the trend: HiPco-D > SG65-D > P2-D. The electrophoretic mobility (EPM) and hydrodynamic diameter of SWCNTs remained unaffected by SWCNT type, pH, and presence of natural organic matter (NOM); nevertheless, the ionic strength (IS) and ion valence (K^+, Ca^{2+}) altered the hydrodynamic diameter and EPM properties of SWCNTs. Overall, it was concluded that the different synthetic approaches resulted in unique breakthrough trends, which were related to metal content (Chowdhury et al. 2012).

Table 5 Physico-chemical characteristics of silica NMs in the UCLA library

Silica NM	Size (nm)			Zeta potential (mV)		
	H_2O	BEGM (2 mg/mL BSA)	DMEM (10% FCS)	H_2O	BEGM (2 mg/mL BSA)	DMEM (10% FCS)
As prepared Stöber silica	118.4 ± 1.9	257.6 ± 22.6	196.7 ± 11.7	−39.2 ± 1.4	−5.5 ± 3.5	−25.2 ± 14.1
Stöbercalcinated at 600 °C	156.6 ± 3.2	282.6 ± 3.2	227.8 ± 0.9	−26.8 ± 0.5	−8.5 ± 4.1	−10.9 ± 2.4
Stöbercalcinated at 800 °C	211.0 ± 6.2	311.9 ± 7.1	233.2 ± 3.6	−34.9 ± 1.6	−10.7 ± 2.8	−5.7 ± 2.8
Rehydrated Stöber silica	143.3 ± 3.8	249.9 ± 2.2	203.6 ± 4.7	−36.8 ± 2	−9.6 ± 4.4	−11.0 ± 6.9
Aggregated Stöber silica	148.1 ± 2.1	532.8 ± 27.8	231.2 ± 2.3	−8.81 ± 0.1	−9.04 ± 1.7	−11.24 ± 1.5
As received fumed silica	131.5 ± 0.6	627.6 ± 69.9	256.3 ± 19	−22.4 ± 7.1	−4.5 ± 3.1	−10.1 ± 8.5
Fumed silica calcinated at 600 °C	286.2 ± 22.5	667.3 ± 23.6	326.3 ± 3.9	−33.2 ± 3.7	−11.5 ± 4.9	−4.9 ± 2.2
Fumed silica calcinated at 800 °C	310.1 ± 11.2	676.7 ± 32.8	339.0 ± 9.9	−19.0 ± 1.6	−7.1 ± 1.2	−4.1 ± 1.7
Rehydrated fumed silica	161.6 ± 29	623.3 ± 18.6	264.4 ± 7.3	−40.5 ± 2.2	−10.7 ± 1.5	−6.5 ± 2.1
Aggregated fumed silica	263.3 ± 7.8	409.3 ± 43.2	248.6 ± 12.8	−58.0 ± 1.3	−0.9 ± 7.9	−2.1 ± 10.9
Mesoporous silica	235.0 ± 7.2	364.8 ± 128.4	362.9 ± 51.1	−43.9 ± 3.6	−18.4 ± 8.7	−4.8 ± 13.1
Min-U-Sil quartz	94.3 ± 5.5	246.1 ± 35.9	126.8 ± 8.0	−15.5 ± 0.3	−19.3 ± 1.6	−7.74 ± 0.3

From Zhang et al. (2012a, b)

Table 6 Physical Characterization of different single-walled carbon nanotubes

	Diameter range (nm)[a]	Length (nm)[b]	Metal mass (%)[c]	Species[c]	Species mass (%)[c]	Metal species (%)[c]
HiPco-D	0.696–1.129	383 ± 281	6.52	Fe	6.52	100
SG65-D	0.682–0.981	449 ± 316	1.80	Co	0.22	12.26
				Mo	1.58	87.74
P2-D	1.158–1.699	404 ± 221	0.21	Y	0.06	30.24
				Ni	0.15	69.76

From Chowdhury et al. (2012)

[a]The diameters of SWCNTs are determined by vis-NIR and TEM

[b]Lengths of SWCNTs were determined from atomic force microscopy

[c]Residual metal species and mass determined via inductively coupled plasma atomic emission spectroscopy

3.5 Combinatorial Synthesis of (Biodegradable) Polymers

Intensive research related to nanomedicine and nanosafety assessment is also evolving. For instance, combinatorial techniques are widely used in the pharmaceutical industry, and are increasingly being applied to the development of polymer coatings. A combinatorial synthesis of biodegradable polyanhydride film and NM libraries as well as the high-throughput detection of protein release from these libraries has recently been reported (Petersen 2012). The method enables the rapid construction of micro-scale polymer libraries, reducing the batch size while creating multivariant polymer systems. Moreover, the combinatorial polymer library can be fabricated into blank or protein-loaded geometries upon dissolution of the polymer library in a solvent and precipitation into a non-solvent (for NMs) or by vacuum drying (for films). The libraries have been screened for protein release kinetics, stability and antigenicity; in vitro cellular toxicity, cytokine production, surface marker expression, adhesion, proliferation and differentiation; and in vivo biodistribution and mucoadhesion (Petersen 2012 and references therein). Such approaches are very promising regarding the development of systematically varied NM libraries and their evaluation.

4 Gap Between Measured Physico-chemical Parameters and Calculated QSAR Descriptors

Given the dynamic nature of NMs, and their context-dependence, there is a disconnect between the physico-chemical parameters characterised routinely and those utilised in QSAR models (Valsami-Jones 2015). Indeed there is still considerable variability in the various lists of minimal characterisation parameters that have been discussed over the last 10 years (see Stefaniak 2013 for a review of these lists) and their degree of overlap. A recent editorial in ACS Nano described this succinctly:

"*Structure-activity analyses of well-characterized material libraries (used for exploring a series of nano/bio interfaces) have elucidated nanoscale-specific properties that go beyond the traditional lists of intrinsic and extrinsic property characterization*" (Nel 2015). Examples of novel or non-traditional characteristics or descriptors linked to novel toxicities include band gap and hydration energies which have been linked to generation of oxidative stress in bacteria and mammalian cells by metal oxide semiconductor materials (Zhang 2012b); surface strain resulting from highly reactive silanols leading to membrane damage by pyrolytic silica (Zhang 2012a), or unfolding of proteins at the NM surface leading to activation of inflammatory receptors (Deng 2011). Examples related to the occurrence of dynamic changes or interactions (which have been termed extrinsic effects) include the complexation of structural cellular phosphate residues on the surface of rare earth oxides and up-conversion NP leading to lysosome damage (Li 2014); and the degradation of surface coatings attached to NMs in the acidic lysosomal environment, leading to lysosomal injury (Wang 2015). As pointed out by Nel et al., none of these structure-activity relationships could have been predicted using the traditional list of intrinsic and extrinsic property evaluations (Nel 2015). To further illustrate this point, we have reviewed the QSAR literature and extracted the descriptors that were used as the basis of predictive models compared to those physico-chemical parameters of the NMs that were characterised, with very clear divergence and discrepancies apparent (See Table 7). Thus, we either need to develop models utilising the easily measured physico-chemical parameters, find ways to extract more useful data from the traditional methods, or develop approaches to routinely measure those parameters more directly linked to structure-activity relationships.

As evident from this snapshot of QSAR models for NMs, most models are based on calculated parameters that take no or limited account of the NMs characteristics in the exposure medium or are derived from crystallographic data (for example) (Puzyn et al. 2011) and are certainly not reliant on detailed physico-chemical characterisation of the dynamics of NM behaviour in the biological medium and organism. More recent efforts include extraction of detailed parameters from TEM images (e.g. Gajewicz 2015) or protein adsorption to the NMs (e.g. Liu 2015a) which are experimentally determined parameters, although corona characterisation is not yet a routine characterisation or required as part of regulatory dossiers for NMs, in large part due to the cost involved and the early stages in terms of verification of a predictive relationship for NM uptake/toxicity. Figure 10 shows an example utilising a calculated version of acid-base properties, which increased with the number of oxygens in the oxide NM and proportion of surface molecules to molecules in volume as descriptors to model NM toxicity to bacteria (Sizochenko 2014). As available datasets increase in number and size, models comparing increasingly diverse NMs and exposure conditions are becoming available, suggesting that significant progress is being made in this arena, although there is still a need for concerted effort in this research field.

It is clear that there is a need for development of a strategy for identification of NMs' critical properties linked to biological impacts, and in particular to tease out

Table 7 Summary of selected QSAR studies from the literature highlighting the physico-chemical parameters measured and the calculated descriptors

NMs used	End-point and biological system	Physico-chemical properties characterised	Calculated descriptors	References
17 nano-metal oxides	Toxicity to *E. coli* bacteria	No NM characterisation Crystallographic data used to calculate 12 structural characteristics EC_{50} determined experimentally and calculated from model	ΔH_{Me+}, which represents enthalpy of formation of a gaseous cation having the same oxidation state as that in the metal oxide structure Structural parameters: • Standard heat of formation of the oxide cluster • Total energy of the oxide cluster • Electronic energy of oxide cluster • Core-core repulsion energy of oxide cluster • Area of oxide cluster calculated based on COSMO • Volume of oxide cluster calculated based on COSMO • Energy of HOMO • Energy of LUMO • Energy difference between HOMO and LUMO • Enthalpy of detachment of metal cations(Me^{n+}) from cluster surface • Enthalpy of formation of a gaseous cation • Lattice energy of oxide	Puzyn et al. (2011)
17 or 18 metal oxide NPs	Cytotoxicity to *E. coli* and HaCaT cells	NP size NP agglomerate size	A combination of simple descriptors which reflect NPs' structure for the different levels of organization: from a single metal oxide molecule (i.e.	Sizochenko (2014)

(continued)

Table 7 (continued)

NMs used	End-point and biological system	Physico-chemical properties characterised	Calculated descriptors	References
			chemical structure) to a supramolecular ensemble of molecules (i.e. nanoparticle size). Liquid Drop model used for NP size. Distinction between interactions of surface versus internal atoms. Parameters to describe metal ion's affinity to biochemical ligands: covalent index (CI) and cation polarizing power (CPP). RF modeling obtained 6 significant descriptors for HaCaT keratinocytes and 7 descriptors for *E. coli*. Descriptors S1, rw, ρ are the same for both models (see Fig. 10)	
229 NPs/cases from literature, 32 diverse chemistries	Toxicity against 1 out of 50 biological targets (b_t) with different complexities (algae, bacteria, cell lines, crustaceans, plants, fish, and others)	Some NPs reported in their bare forms, while other NPs were coated by different organic molecules, specifically using 12 different coating agents (s_c) NP size (L) based on experimental data	4 different descriptors namely: • molar volume (V) • electronegativity (E) • polarizability (P) • NP size (L) Three descriptors were extracted from the public source Chemical Periodic Table (Hsu 2013) These were not predictive so new descriptors were calculated, for example:	Kleandrova (2014)

(continued)

Table 7 (continued)

NMs used	End-point and biological system	Physico-chemical properties characterised	Calculated descriptors	References
			• TEi(cj)rf a binary (classification) variable expressing the toxic effect of the NP used as reference • ΔΔE(bt) a perturbation term that describes changes in the electronegativity between new (output or final state) NM and the other used as reference, also depending on the biological targets (9 such descriptors in total)	
300 NPs/cases retrieved from public source OChem	Anti-bacterial activity using range of assays in up to 34 bacterial strains NPs classified as active or inactive	Data from database • NP size • NP shape • NP surface coating (15 different) Molar volume (AMV), Electronegativity (AE) and Polarizability (AP), retrieved from website Chemical Periodic Table	Mixed NPs calculated as sum of properties/number of atoms Chemical structures of coating agents computed: • spectral moments of bond adjacency matrix, weighted by properties such as standard bond distance, the atomic polar surface area and the atomic refractivity	Speck-Planche (2015)
18 nano-metal oxides	Toxicity to human keratinocyte (HaCaT) cell line as a model for dermal exposure.	TEM and DLS for NP size	Calculated a set of 27 parameters quantitatively describing variability of NPs' structure—nano-descriptors including: 16 quantum-mechanical descriptors, i.e.	Gajewicz (2015)

(continued)

Table 7 (continued)

NMs used	End-point and biological system	Physico-chemical properties characterised	Calculated descriptors	References
	Comparison of NP toxicity to eukaryotic system (HaCaT) and the prokaryotic system (*E. coli*)		• Total energy • Electronic energy, • Core–core repulsion energy, • Solvent accessible-surface, • Energy of HOMO • Energy of LUMO • Chemical hardness, • Total softness, • HOMO-LUMO energy gap, • Electronic chemical potential, • Valance band, • Conduction band 11 image descriptors (derived from TEM images)—Area, Volume, Surface diameter, Volume/mass diameter, Volume/surface area, Aspect ratio X, Aspect ratio Y, Porosity X, Porosity Y, Circularity, Sphericity	
Metal oxide nanoparticles	Photo-induced cytotoxicity to bacteria *Escherichia coli*	NPs represented as molecular input-line entry system (SMILES)	Quasi-SMILES is the representation of data on molecular structure together with condition: presence or absence of photo-inducing. The presence of photo-inducing indicated by symbol '^' that is added at the end of traditional SMILES	Toropova (2015)

(continued)

Table 7 (continued)

NMs used	End-point and biological system	Physico-chemical properties characterised	Calculated descriptors	References
105 surface modified Gold NPs utilising 67 different surface ligands	Dataset of cellular association of 84 Au NPs from Liu (2015a)	39 physico-chemical properties of the Au NPs (as synthesized and with serum) including TEM and DLS size characterization, zeta potential, absorbance spectrophotometry, and the amount of adsorbed serum protein on the NP surface obtained from the bicinchoninic acid (BCA) assay	Both linear and nonlinear (ε-SVR) regressions used for cellular association of Au NPs. The regressions were coupled with sequential forward floating selection to identify suitable QSAR descriptors from the three descriptor sets, including 120 protein corona fingerprints, 19 of the nanoparticle properties, and a composite of the two sets	Liu (2015a)
Iron oxide core with different surface-modifying organic molecules	Cellular uptake	Unknown	11 found predictive in linear model 6 predictive in non-linear model	Liu (2015b)

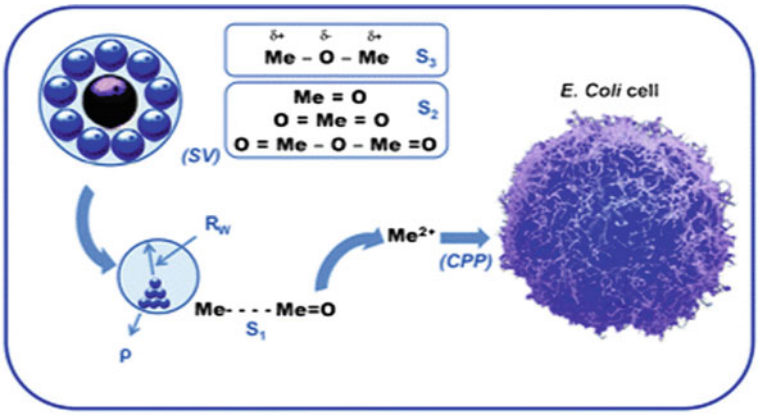

Fig. 10 Schematic representation of the mechanism of metal oxide nanoparticle toxicity for *E. coli* cells. From Sizochenko (2014). The important descriptors for *E. coli* cytotoxicity of the metal oxide NMs were determined to be: S_1 unbonded two-atomic fragments [Me]· · ·[Me], which were encoded based on SiRMS-derived descriptors, encoding the distance where the potential reaches minimum at van der Waals interactions (7%); r_w Wigner–Seitz radius (22%); ρ mass density (2%); *CPP*, cation polarizing power (30%); S_2 SiRMS-derived electronegativity aligned descriptor of oxides molecules—in a sense the acid–base property of oxides. This parameter increases with the number of oxygen atoms in a molecule (3%); S_3 tri-atomic fragments [Me]–[O]–[Me], which were encoded by SiRMS-derived descriptors, encoding electronegativity (29%); and *SV*, the proportion of surface molecules to molecules in volume (7%). % is used to represent the absolute impacts for each descriptor

the various pathways involved. One potential starting point is to link with the emerging Adverse Outcome Pathways (AOP) approach, which aims to identify so-called molecular initiating events (MIE) and follow these through the subsequent effects to adverse outcomes and cellular, organismal, community and population levels. Initial conceptualization for nanotoxicology is already underway (Gerloff 2016), and a case study of liver toxicity proposed that the differences between NM and chemically-induced adversity were primarily related to differences in toxicokinetics and the nature of the initial Key Events in the AOP. NM reactivity was associated with the NM's potential to generate oxidative stress, determined as the ability of the NMs to exchange electrons with biological redox species in the cell (Gerloff 2016). The model was tested using the metal oxide libraries described in Table 5 (Zhang 2012) and was only partially accurate in predicting the capacity of metal oxide NMs to induce oxidative stress, since other metal oxide NMs induce similar effects through ion dissolution, illustrating the importance of relating QSAR properties to proposed MIEs (Gerloff 2016). Thus, teasing out the relative contributions of different NM physico-chemical parameters to specific MIEs, and grouping of NMs based on all properties that link to specific MIEs might be a useful way forward. One proposal of how to do such a mapping of the partial contributions of multiple parameters to a specific endpoint was proposed by Lynch et al., using principle components analysis which could then be complemented with factorial

analysis to determine contributions to the different modes of action (Lynch et al. 2014a). The commonality of NM physico-chemical parameters confirmed to contribute across the different modes of action shown in Table 2 shows the scale of the computational and experiment challenge, and highlights the need for much closer cooperation between the two approaches, and the need for involvement of modellers in co-designing experimental studies to ensure they provide the full spectrum of temporal and spatial datasets needed for computational and in silico approaches.

5 Conclusions

This chapter summarises the current state of the art in terms of mechanisms of NM toxicity, in light of the emerging understanding of the context-dependence of physico-chemical characteristics of NMs that may be specifically linked to their toxicity. In addition, the chapter summarises some of the challenges for defining and regulating NMs, and in particular for developing predictive read-across tools including QSARs/QPARs, which result from the fact that NMs are a highly diverse and highly dynamic group of materials. While there is growing consensus that many of the biological effects from manufactured or engineered NMs may not be all that different from ultrafine anthropogenic particles of similar compositions, it is clear that the variety of materials that can be engineered at the nanoscale, and the variety of forms (shapes, structures, morphologies, composites and hybrids etc.) that can be produced opens up significantly more challenges than arise from combustion-related particles.

In particular, the current state of the art in terms of NM libraries with accompanying physico-chemical characterisation and uptake or toxicity datasets available in the literature that can be used as the basis for development of QSARs/QPARs is presented. Building on this, some initial progress towards QSAR models was presented, and the challenges and ongoing disconnect between measured properties and those found to be predictive in QSARs, which are almost entirely calculated, often entirely independently from the measured datasets was discussed.

An ongoing challenge for the field is that access to the NMs themselves for additional experimentation/validation is generally limited outside the group that produced the NMs. Thus, it would be valuable for journals to require that NMs underpinning datasets be made available for sharing upon request or placement of samples in a repository, although there are significant cost challenges associated with this, as well as issues related to NMs ageing and evolution. However, it is unlikely that the costs would be more significant than those associated with protein synthesis or development of transgenic animal models, so approaches could be adopted from these fields alternatively. An alternative would be that full SOPs for production of the NMs be published (or included as part of the supplementary information) and detailed accompanying characterisation information (including

SOPs, instrument details and calibrations), and that authors are provided with facilities for cross-checking of outputs by the original NM-library developer, as part of the publication requirements for NMs datasets.

Acknowledgements This work was funded via the European Commission's 7th Framework Programme project "NanoMILE" (Contract N°. NMP4-LA-2013-310451). The authors acknowledge the NanoMILE consortium for constructive discussions.

References

Ahmadi, T. S., Wang, Z. L., Green, T. C., Henglein, A., & El-Sayed, M. A. (1996). Shape-controlled synthesis of colloidal platinum nanoparticles. *Science*, *272*, 1924–1925.

Albanese, A., Walkey, C. D., Olsen, J. B., Guo, H., Emili, A., & Chan, W. C. (2014). Secreted biomolecules alter the biological identity and cellular interactions of nanoparticles. *ACS Nano, 8,* 5515–5526.

Baun, A., Sørensen, S. N., Rasmussen, R. F., Hartmann, N. B., & Koch, C. B. (2008). Toxicity and bioaccumulation of xenobiotic organic compounds in the presence of aqueous suspensions of aggregates of nano-C(60). *Aquatic Toxicology, 86,* 379–387.

Bexiga, M. G., Varela, J. A., Wang, F., Fenaroli, F., Salvati, A., Lynch, I., et al. (2011). Cationic nanoparticles induce caspase 3-, 7- and 9-mediated cytotoxicity in a human astrocytoma cell line. *Nanotoxicology, 5,* 557–567.

Brus, L. (1994). Luminescence of silicon materials: Chains, sheets, nanocrystals, nanowires, microcrystals, and porous silicon. *Journal of Physical Chemistry, 98,* 3575–3581.

Burello, E., & Worth, A. P. (2011). A theoretical framework for predicting the oxidative stress potential of oxide nanoparticles. *Nanotoxicology, 5,* 228–235.

Bussy, C., Pinault, M., Cambedouzou, J., Landry, M. J., Jegou, P., Mayne-L'hermite, M., et al. (2012). Critical role of surface chemical modifications induced by length shortening on multi-walled carbon nanotubes-induced toxicity. *Particle and Fibre Toxicology, 9,* 46.

Chng, E. L., & Pumera, M. (2013). The toxicity of graphene oxides: Dependence on the oxidative methods used. *Chemistry, 19,* 8227–8235.

Chowdhury, I., Duch, M. C., Gits, C. C., Hersam, M. C., & Walker, S. L. (2012). Impact of synthesis methods on the transport of single walled carbon nanotubes in the aquatic environment. *Environmental Science and Technology, 46,* 11752–11760.

Clemments, A. M., Botella, P., & Landry, C. C. (2015). Protein adsorption from biofluids on silica nanoparticles: Corona analysis as a function of particle diameter and porosity. *ACS Applied Materials & Interfaces, 7,* 21682–21689.

Dawson, K. A., Linse, S., & Lynch, I. (2007). Water as a mediator of protein-nanoparticle interactions: Entropy driven protein binding as a paradigm for protein therapeutics in the Biopharma industry? *E-nano Newsletter [Online],* 23–34.

Deng, Z. J., Liang, M., Monteiro, M., Toth, I., & Minchin, R. F. (2011). Nanoparticle-induced unfolding of fibrinogen promotes Mac-1 receptor activation and inflammation. *Nature Nanotechnology, 6,* 39–44.

Deng, Z. J., Liang, M., Toth, I., Monteiro, M., & Minchin, R. F. (2013). Plasma protein binding of positively and negatively charged polymer-coated gold nanoparticles elicits different biological responses. *Nanotoxicology, 7,* 314–322.

Fadeel, B., Feliu, N., Vogt, C., Abdelmonem, A. M., & Parak, W. J. (2013). Bridge over troubled waters: understanding the synthetic and biological identities of engineered nanomaterials. *Wiley Interdisciplinary Reviews: Nanomedicine and Nanobiotechnology, 5,* 111–129.

Gajewicz, A., Schaeublin, N., Rasulev, B., Hussain, S., Leszczynska, D., Puzyn, T., et al. (2015). Towards understanding mechanisms governing cytotoxicity of metal oxides nanoparticles: Hints from nano-QSAR studies. *Nanotoxicology, 9,* 313–325.

George, S., Lin, S. J., Jo, Z. X., Thomas, C. R., Li, L. J., Mecklenburg, M., et al. (2012). Surface defects on plate-shaped silver nanoparticles contribute to its hazard potential in a fish gill cell line and zebrafish embryos. *ACS Nano*, *6*, 3745–3759.

Gerloff, K., Landesmann, B., Worth, A., Munn, S., Palosaari, T., & Whelan, M. (2016). The adverse outcome pathway approach in nanotoxicology. *Computational Toxicology*.

Harper, S. L., Carriere, J. L., Miller, J. M., Hutchinson, J. E., Maddux, B. L. S., & Tanguay, R. L. (2011). Systematic evaluation of nanomaterial toxicity: Utility of standardised materials and rapid assays. *ACS Nano, 5,* 4688–4697.

Hassellöv, M., & Kaegi, R. (2009). Analysis and characterization of manufactured nanoparticles in aquatic environments. In J. R. Lead & E. Smith (Eds.), *Environmental and human health impacts of nanotechnology.*

Ho, C.-M., Yau, S. K.-W., Lok, C.-N., So, M.-H., & Che, C.-M. (2010). Oxidative dissolution of silver nanoparticles by biologically relevant oxidants: A kinetic and mechanistic study. *Chemistry—An Asian Journal, 5,* 285–293.

HSU, D. D. (2013). Chemical periodic table. http://www.chemicool.com/.

Ivask, A., Suarez, E., Patel, T., Boren, D., Ji, Z. X., Holden, P., et al. (2012). Genome-wide bacterial toxicity screening uncovers the mechanisms of toxicity of a cationic polystyrene nanomaterial. *Environmental Science and Technology, 46,* 2398–2405.

Kleandrova, V. V., Luan, F., González-Díaz, H., Ruso, J. M., Speck-Planche, A., & Cordeiro, N. D. S. (2014). Computational tool for risk assessment of nanomaterials: Novel QSTR-perturbation model for simultaneous prediction of ecotoxicity and cytotoxicity of uncoated and coated nanoparticles under multiple experimental conditions. *Environmental Science and Technology, 48,* 14686–14694.

Klein, J. (2007). Probing the interactions of proteins and nanoparticles. *PNAS, 104,* 2029–2030.

Lee, K. J., Browning, L. M., Nallathamby, P. D., & Xu, X. H. (2013). Study of charge-dependent transport and toxicity of Peptide-functionalized silver nanoparticles using zebrafish embryos and single nanoparticle plasmonic spectroscopy. *Chemical Research in Toxicology, 26,* 904–917.

Li, R., Ji, Z., Chang, C. H., Dunphy, D. R., Cai, X., Meng, H., et al. (2014). Surface interactions with compartmentalized cellular phosphates explain rare earth oxide nanoparticle hazard and provide opportunities for safer design. *ACS Nano*, *8*, 1771–1783.

Li, Y., Zhang, W., Niu, J., & Chen, Y. (2013). Surface coating-dependent dissolution, aggregation, and ROS generation of silver nanoparticles under different irradiation conditions. *Environmental Science and Technology, 47,* 10293–10301.

Lin, S., Zhao, Y., Ji, Z., et al. (2013). Zebrafish high-throughput screening to study the impact of dissolvable metal oxide nanoparticles on the hatching enzyme, ZHE1. *Small (Weinheim an der Bergstrasse, Germany) 9,* 1776–1785. doi:10.1002/smll.201202128.

Linsinger, T., Roebben, G., Gilliland, D., Calzolai, L., Rossi, F., Gibson, N., et al. (2012). Requirements on measurements for the implementation of the European Commission definition of the term "nanomaterial". *Report EUR 25404 EN*.

Liu, J., Aruguete, D. M., Jinschek, J. R., Rimstidt, J. D., & Hochella, Jr., M. F. (2008). The non-oxidative dissolution of galena nanocrystals: Insights into mineral dissolution rates as a function of grain size, shape, and aggregation state. *Geochimica et Cosmochimica Acta*, *72*, 5984–5996.

Liu, J., von der Kammer, F., Zhang, B., Legros, S., & Hofmann, T. (2013a). Combining spatially resolved hydrochemical data with in-vitro nanoparticle stability testing: Assessing environmental behavior of functionalized gold nanoparticles on a continental scale. *Environment International, 59,* 53–62.

Liu, R., Jiang, W., Walkey, C. D., Chan, W. C., & Cohen, Y. (2015a). Prediction of nanoparticles-cell association based on corona proteins and physicochemical properties. *Nanoscale, 7,* 9664–9675.

Liu, R., Rallo, R., Bilal, M., & Cohen, Y. (2015b). Quantitative structure-activity relationships for cellular uptake of surface-modified nanoparticles. *Combinatorial Chemistry & High Throughput Screening, 18,* 365–375.

Liu, R., Rallo, R., George, S., Ji, Z., Nair, S., Nel, A. E., et al. (2011). Classification NanoSAR development for cytotoxicity of metal oxide nanoparticles. *Small, 7,* 1118–1126.

Liu, X., Chen, G., Keller, A. A., & Su, C. (2013b). Effects of dominant material properties on the stability and transport of TiO_2 nanoparticles and carbon nanotubes in aquatic environments: From synthesis to fate. *Environmental Science: Processes Impacts, 15*, 169–189.

Lövestam, G., Rauscher, H., Roebben, G., Sokull Klüttgen, B., Gibson, N., Putaud, J.-P., et al. (2010). Considerations on a definition of nanomaterial for regulatory purposes.

Lowry, G. V., Gregory, K. B., Apte, S. C., & Lead, J. R. (2012). Transformations of nanomaterials in the environment. *Environmental Science and Technology, 46,* 6893–6899.

Lowry, G. V., Hill, R. J., Harper, S., Rawle, A. F., Hendren, C. O., Klaessig, F., et al. (2016). Guidance to improve the scientific value of zeta-potential measurements in nanoEHS. *Environmental Science: Nano, 3,* 953–965.

Lynch, I. (2007). Are there generic mechanisms governing interactions between nanoparticles and cells? Epitope mapping the outer layer of the protein-material interface. *Physica A—Statistical Mechanics and its Applications, 373,* 511–520.

Lynch, I., Dawson, K. A., Lead, J. R., & Valsami-Jones, E. (2014a). Macromolecular coronas and their importance in nanotoxicology and nanoecotoxicology. In J. R. Lead & E. Valsami-Jones (Eds.), *Nanoscience and the environment.*

Lynch, I., Weiss, C., & Valsami-Jones, E. (2014b). A strategy for grouping of nanomaterials based on key physico-chemical descriptors as a basis for safer-by-design NMs. *Nano Today, 9,* 266–270.

Melagraki, G., & Afantitis, A. (2014). Enalos InSilicoNano Platform: An online decision support tool for the design and virtual screening of nanoparticles. *RSC Advances, 4,* 50713–50725.

Melagraki, G., & Afantitis, A. (2015). A risk assessment tool for the virtual screening of metal oxide nanoparticles through Enalos InSilicoNano Platform. *Current Topics in Medicinal Chemistry*, *15*, 1827–1836.

Meng, H., Xia, T., George, S., & Nel, A. E. (2009). A predictive toxicological paradigm for the safety assessment of nanomaterials. *ACS Nano, 3,* 1620–1627.

Merhi, M., Dombu, C. Y., Brient, A., Chang, J., Platel, A., le Curieux, F., et al. (2012). Study of serum interaction with a cationic nanoparticle: Implications for in vitro endocytosis, cytotoxicity and genotoxicity. *International Journal of Pharmaceutics, 423,* 37–44.

Misra, S. K., Dybowska, A., Berhanu, D., Luoma, S. N., & Valsami-Jones, E. (2012). The complexity of nanoparticle dissolution and its importance in nanotoxicological studies. *Science of the Total Environment, 438,* 225–232.

Nap, R. J., & Szleifer, I. (2013). How to optimize binding of coated nanoparticles: Coupling of physical interactions. *Molecular Organization and Chemical State Biomaterial Science, 1,* 814–823.

Nel, A. E., Parak, W. J., Chan, W. C., Xia, T., Hersam, M. C., Brinker, C. J., et al. (2015). Where are we heading in nanotechnology environmental health and safety and materials characterization? *ACS Nano, 9,* 5627–5630.

Pagnout, C., Jomini, S., Dadhwal, M., Caillet, C., Thomas, F., & Bauda, P. (2012). Role of electrostatic interactions in the toxicity of titanium dioxide nanoparticles toward Escherichia coli. *Colloids and Surfaces B: Biointerfaces, 92,* 315–321.

Park, E.-J., Yi, J., Kim, Y., Choi, K., & Park, K. (2010). Silver nanoparticles induce cytotoxicity by a Trojan-horse type mechanism. *Toxicology in Vitro, 24,* 872–878.

Petersen, L. K., Chavez-Santoscoy, A. V., & Narasimhan, B. (2012). Combinatorial synthesis of and high-throughput protein release from polymer film and nanoparticle libraries. *Journal of Visualized Experiments, 67,* 3882.

Pokhrel, S., Nel, A. E., & Mädler, L. (2012). Custom-designed nanomaterial libraries for testing metal oxide toxicity. *Accounts of Chemical Research, 46,* 632–641.

Puzyn, T., Rasulev, B., Gajewicz, A., Hu, X., Dasari, T. P., Michalkova, A., et al. (2011). Using nano-QSAR to predict the cytotoxicity of metal oxide nanoparticles. *Nature Nanotechnology*, *6*, 175–178.

Salvati, A., Aberg, C., dos Santos, T., Varela, J., Pinto, P., Lynch, I., et al. (2011). Experimental and theoretical comparison of intracellular import of polymeric nanoparticles and small molecules: Toward models of uptake kinetics. *Nanomedicine, 7,* 818–826.

Sau, T. K., & Murphy, C. J. (2004). Room temperature, high-yield synthesis of multiple shapes of gold nanoparticles in aqueous solution. *Journal of the American Chemical Society, 126,* 8648–8649.

Sau, T. K., Urban, A. S., Dondapati, S. K., Fedoruk, M., Horton, M. R., Rogach, A. L., et al. (2009). Controlling loading and optical properties of gold nanoparticles on liposome membranes. *Colloids and Surfaces A—Physicochemical and Engineering Aspects, 342,* 92–96.

Shaw, S. Y., Westly, E. C., Pittet, M. J., Subramanian, A., Schreiber, S. L., & Weissleder, R. (2008). Perturbational profiling of nanomaterial biologic activity. *Proceedings of the National Academy of Sciences U.S.A., 105*, 7387–7392.

Sizochenko, N., Rasulev, B., Gajewicz, A., Kuz'Min, V., Puzyn, T., & Leszczynski, J. (2014). From basic physics to mechanisms of toxicity: The "liquid drop" approach applied to develop predictive classification models for toxicity of metal oxide nanoparticles. *Nanoscale, 6,* 13986–13993.

Soler, M. A. G., Lima, E. C. D., da Silva, S. W., Melo, T. F. O., Pimenta, A. C. M., Sinnecker, J. P., et al. (2007). Aging investigation of cobalt ferrite nanoparticles in low pH magnetic fluid. *Langmuir, 23,* 9611–9617.

Speck-Planche, A., Kleandrova, V. V., Luan, F., & Cordeiro, M. N. D. S. (2015). Computational modeling in nanomedicine: Prediction of multiple antibacterial profiles of nanoparticles using a quantitative structure-activity relationship perturbation model. *Nanomedicine, 10,* 193–204.

Stamm, H. (2011). Risk factors: Nanomaterials should be defined. *Nature, 476,* 399.

Stefaniak, A. B., Hackley, V. A., Roebben, G., Ehara, K., Hankin, S., Postek, M. T., et al. (2013). Nanoscale reference materials for environmental, health and safety measurements: Needs, gaps and opportunities. *Nanotoxicology, 7,* 1325–1337.

Studer, A. M., Limbach, L. K., van Duc, L., Krumeich, F., Athanassiou, E. K., Gerber, L. C., et al. (2010). Nanoparticle cytotoxicity depends on intracellular solubility: Comparison of stabilized copper metal and degradable copper oxide nanoparticles. *Toxicology Letters, 197,* 169–174.

Sund, J., Alenius, H., Vippola, M., Savolainen, K., & Puustinen, A. (2011). Proteomic characterization of engineered nanomaterial–protein interactions in relation to surface reactivity. *ACS Nano, 5,* 4300–4309.

Teoh, W. Y., Amal, R., & Madler, L. (2010). Flame spray pyrolysis: An enabling technology for nanoparticles design and fabrication. *Nanoscale, 2,* 1324–1347.

Toropova, A. P., Toropov, A. A., Rallo, R., Leszczynska, D., & Leszczynski, J. (2015). Optimal descriptor as a translator of eclectic data into prediction of cytotoxicity for metal oxide nanoparticles under different conditions. *Ecotoxicology and Environmental Safety, 112,* 39–45.

Tsuzuki, T. (2009). Commercial scale production of inorganic nanoparticles. *International Journal of Nanotechnology* (IJNT), *6*. doi:10.1504/IJNT.2009.024647.

Vácha, R., Martinez-Veracoechea, F. J., & Frenkel, D. (2011). Receptor-mediated endocytosis of nanoparticles of various shapes. *Nano Letters, 11,* 5391–5395.

Valsami-Jones, E., & Lynch, I. (2015). How safe are nanomaterials? *Science, 350,* 388–389.

von der Kammer, F., Ferguson, P. L., Holden, P. A., Masion, A., Rogers, K. R., Klaine, S. J., et al. (2012). Analysis of engineered nanomaterials in complex matrices (environment and biota): General considerations and conceptual case studies. *Environmental Toxicology and Chemistry, 31,* 32–49.

Walczyk, D., Bombelli, F. B., Monopoli, M. P., Lynch, I., & Dawson, K. A. (2010). What the cell "sees" in bionanoscience. *Journal of the American Chemical Society*, *132*, 5761–5768.

Walkey, C. D., Olsen, J. B., Song, F., Liu, R., Guo, H., Olsen, D. W., et al. (2014). Protein corona fingerprinting predicts the cellular interaction of gold and silver nanoparticles. *ACS Nano, 8,* 2439–2455.

Wang, X., Duch, M. C., Mansukhani, N., Ji, Z., Liao, Y. P., Wang, M., et al. (2015). Use of a pro-fibrogenic mechanism-based predictive toxicological approach for tiered testing and decision analysis of carbonaceous nanomaterials. *ACS Nano*, *9*, 3032–3043.

Weissleder, J., Kelly, K, Sun, E. Y., Shtatland, T., & Josephson, L. (2005). Cell-specific targeting of nanoparticles by multivalent attachment of small molecules. *Nature Biotechnology*, *23*, 1418–1423.

Wells, D. M., Rossi, G., Ferrando, R., & Palmer, R. E. (2015). Metastability of the atomic structures of size-selected gold nanoparticles. *Nanoscale, 7,* 6498–6503.

Xia, T., Meng, H., George, S., Zhang, H., Wang, X., Ji, Z., et al. (2012). Strategy for toxicity screening of nanomaterial. *Material Matters.* http://www.sigmaaldrich.com/technical-documents/articles/materials-science/strategy-for-toxicity-screening-of-nanomaterials.html.

Xia, X.-R., Monteiro-Riviere, N. A., & Riviere, J. E. (2010). An index for characterization of nanomaterials in biological systems. *Nature Nanotechnology, 5,* 671–675.

Yang, S. T., Liu, Y., Wang, Y. W., & Cao, A. (2013). Biosafety and bioapplication of nanomaterials by designing protein–nanoparticle interactions. *Small, 9,* 1635–1653.

Zhang, H., Dunphy, D. R., Jiang, X., Meng, H., Sun, B., Tarn, D., et al. (2012a). Processing pathway dependence of amorphous silica nanoparticle toxicity: Colloidal vs pyrolytic. *JACS, 134,* 15790–15804.

Zhang, H., Ji, Z., Xia, T., Meng, H., Low-Kam, C., Liu, R., et al. (2012b). Use of metal oxide nanoparticle band gap to develop a predictive paradigm for oxidative stress and acute pulmonary inflammation. *ACS Nano, 6,* 4349–4368.

Zheng, H., Mortensen, L. J., & Delouise, L. A. (2013). Thiol antioxidant-functionalized CdSe/ZnS quantum dots: Synthesis, characterization, cytotoxicity. *Journal of Biomedical Nanotechnology, 9,* 382–392.